

REVIEW

Organosilicon Polymers—Synthesis, Architecture, Reactivity and Applications

Robin Richter,* Gerhard Roewer,* Uwe Böhme,* Kathleen Busch,* Florence Babonneau,‡ Hans Peter Martin† and Eberhard Müllert

* Department of Inorganic Chemistry and † Department of Ceramic Materials, Freiberg University of Mining and Technology, Leipziger Str. 29, D-09596 Freiberg, Germany, and ‡ Chimie de la Matière Condensée, Université Pierre et Marie Curie, 4 place Jussieu, F-75252 Paris, Cédex 05, France

Tailoring of polysilanes with given architectures and reactivities is a great challenge in the field of SiC pre-ceramic polymers. This paper reviews recent polysilane and related copolymer synthesis reactions.

It is shown that the Wurtz-type polymerization of dichloro-, trichloro- or tetrachloro-silanes, so far the most extensively studied, enables access to a large variety of architectures ranging from one- to three-dimensional (3D) topologies, and based on secondary $>\text{SiR}_2$, tertiary $\text{RSi}(\text{Si})_3$ or quaternary $\text{Si}(\text{Si})_4$ silicon units in the polymer backbone. These polysilanes usually present an intrinsic low reactivity, detrimental for fiber processing. Examples are given to illustrate how this reactivity can be increased by secondary substitution reactions, which create reactive entities that can favor further cross-linking reactions.

Secondly a novel route involving heterogeneously catalyzed disproportionation of chloromethyldisilanes, developed in our laboratory, is reviewed which offers a direct access to polysilyne-type 3D architecture constituted by arrangements of fused rings. The Lewis-base catalyzed disproportionation mechanism is discussed and seems to involve donor-stabilized silylenes as key intermediates in the polymer formation process. The experimental results are supported by *ab-initio* quantum chemical calculations.

Silylenes attack the Si sites of higher functionality causing a high regioselectivity for the exclusive formation of branched oligosilanes. The oligomers undergo thermally induced branching and crosslinking reactions leading to poly(chloromethylsilane)s. Obvi-

ously, there are analogies to the oligomer and polymer formation of the transition-metal complex catalyzed dehydropolymerization of methyldisilanes. Poly(chloromethylsilane)s exhibit a high reactivity due to the presence of Si–Cl bonds.

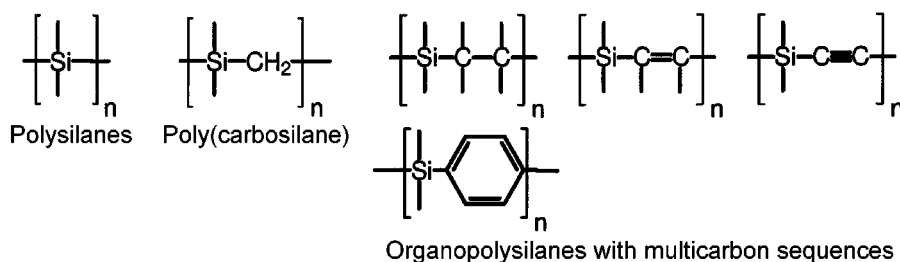
Disproportionation of chloromethyldisilanes in presence of olefins such as styrene provides promising polymer precursors for SiC fibers. Their rheological properties have been investigated for various styrene contents. The polymer fibers spun from melt are cured under ammonia, and then pyrolyzed to silicon carbide fibers, showing temperature resistance up to 1500 °C. © 1997 by John Wiley & Sons, Ltd.

Keywords: polysilane; poly(carbosilane); disilane; oligosilane; SiC fiber; SiC precursor; dehalocoupling; dehydropolymerization; disproportionation

1 INTRODUCTION

Organosilicon polymers, including polysilanes, poly(carbosilane)s or polysilanes containing multicarbon sequences, can be pyrolyzed to afford mixtures of silicon carbide and carbon, or nearly pure SiC (Scheme 1).¹ Over 20 years of intensive research have been concerned with polymer synthesis, processing and pyrolysis methodologies, targeting polymer-derived SiC shapes (fibers, monoliths), layers or powders.^{2,3}

At present the manufacture of well-defined ceramic fibers is still a complex task in pre-



Scheme 1. Characteristic backbone units of organosilicon polymers.

ceramic polymer processing.⁴ Several efforts have been successful in producing phase-pure and fully dense forms of SiC with excellent mechanical properties and thermal resistance.^{5,6} Nevertheless, chemical tailoring of polymer architecture remains a challenge to polymer science, as does the definition of the resulting structure–property relationships. Several objectives must be attained, as:

- *controllable polymer rheology* as an essential requirement for shaping processing (e.g. melt-spinning);
- *adjustable polymer reactivity* to allow the pre-ceramic forms (e.g. polymer fiber) to be rendered infusible before pyrolysis (curing);
- *controllable pyrolytic degradation* into the ceramic materials (e.g. with control of weight loss, excess carbon content, crystallization behavior, shrinkage, mechanical properties, thermal resistance etc.);
- *low cost*.

One reason why the polymer routes to SiC remain highly complex is that the well-defined, high-molecular-weight polysilanes and related polymers are generally kinetic products. They do not correspond to equilibrium states. Competing polymer degradation and formation of thermodynamically stable cyclic oligomers must be taken into consideration, not only during the reaction course, but also during characterization or even processing. Moreover, it is difficult to predict which kinds of polymer architecture will lead to selected ceramic properties under specific pyrolysis conditions, since there is a lack of understanding of the mechanisms whereby polymer crosslinking and degradation reactions occur during pyrolysis.

So far, Wurtz-type dehalocoupling of halo-organosilanes is the most often applied synthetic

method for pre-ceramic polymers. Unfortunately this synthetic approach to Si–Si or Si–C backbones rarely tolerates reactive functionalities. Therefore latent polymer reactivity that might aid further crosslinking reactions (curing), which are essential before pyrolysis, is kept low; introduction of urgently needed polymer reactivity demands additional processing steps, however.

In contrast, catalytic ‘polymerization’ methods such as dehydropolymerization of organo-silanes or -disilanes^{7–12} or disproportionation of halo-organosilanes lead to reactive organosilicon polymers bearing Si–H or Si–Cl groups,¹³ albeit at the cost of introducing additional branching.

This paper summarizes very recent investigations concerning the synthesis of polysilane architecture with 1D to 3D (one- to three-dimensional) topologies. First, in a literature review on recent results concerning dehalocoupling and dehydropolymerization reactions, the polymerization mechanisms are discussed. The polymer structure–property relationships are also illustrated, showing that these polysilanes, by presenting a large range of possible architecture and reactivity, can be modified so as to possess quite different properties, which make possible their application as photoresists, semiconductors or SiC pre-ceramic precursors, for example.

Secondly, we provide an overview of our own investigations concerning the synthesis of reactive poly(chloromethylsilane)s by a novel route: the heterogeneous Lewis-base catalyzed disproportionation of chloromethyldisilanes. A reaction mechanism, based on experimental results as well as *ab-initio* quantum chemical calculations, is discussed. Finally the disproportionation of chloromethyldisilanes in the presence of olefins and the application of the as-prepared polymers as promising SiC fiber precursors are presented.

2 SYNTHESIS ROUTES TO POLYMER BACKBONES OF DIFFERENT REACTIVITY

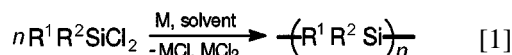
2.1 Reductive coupling reactions

2.1.1 Polymer architecture

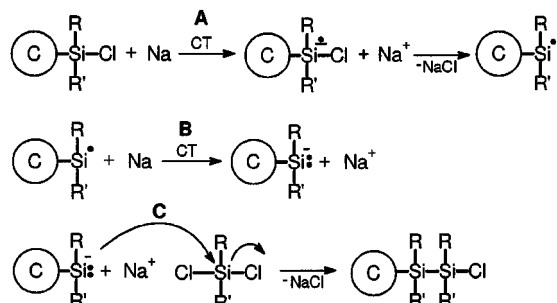
Silicon-based building blocks in organosilicon polymers can be encountered in a variety of 1D to 3D topologies involving chains, branched chains or ordered or disordered networks. While the synthesis of 1D (linear) polysilylenes has been extensively investigated and comprehensively surveyed several times,^{14–21} more recent investigations focus on tailoring 2D or 3D branched and network polymers. Nevertheless several new aspects of the preparation of polysilylenes remain worthy of consideration, as discussed below.

2.1.2 Linear polymers

Linear Si–Si catenations (polysilylenes) are typically prepared by alkali-metal reductive coupling of dichloro-organosilanes $R^1R^2SiCl_2$ in hydrocarbon solvents.¹⁴



Synthesis of high-molecular-weight polysilylenes with narrow molecular weight distributions and polydispersities is still difficult to achieve. A closer inspection of the dehalocoupling mechanism, which is not understood in detail so far, gives an insight into the complex reaction system. The polymerization is assumed to be a chain-growth process, i.e. a sequence of slow initiation, fast propagation and termination steps.¹⁸ Chain-growth, as depicted in Scheme 2, will proceed when monomer and polymer chain-ends possess different reactivities: the electron affinity of the Si–Cl bond on end groups

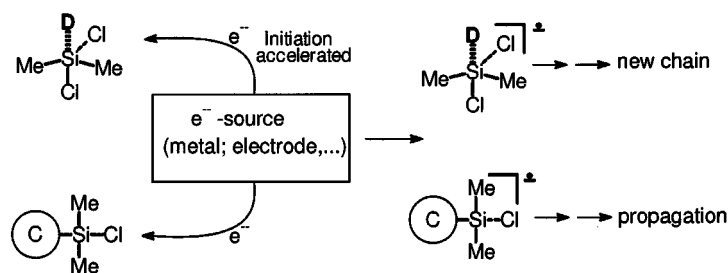


Scheme 2. Proposed chain-propagation mechanism of reductive coupling of halosilanes.

increases along with chain length.¹⁸ Consequently single e^- -transfers (**A** and **B**) from the alkaline metal are favored on end groups rather than on monomers. The charge of the as-formed silyl anion can be delocalized due to Si–Si σ -conjugation.¹⁴ Finally, since the monomer is more electrophilic towards the polymeric silyl anion than another Si–Cl end group, the chain propagates by nucleophilic substitution (S_N2) (**C**) at the monomer.²² Usually a trimodal weight distribution is observed using alkali-metal (sodium) dehalocoupling: the low-molecular-weight fraction consists of cyclosilanes mainly with four-, five- and six-membered rings, the second fraction contains a mixture of lower-molecular-weight ($<10\,000$) and the highest fraction consists of higher-molecular-weight ($>100\,000$) polymers.^{14,23} Cyclosilanes are probably formed either by intramolecular cyclization reactions of oligomeric tetra-, penta- or hexasilanes containing both Si–Cl and silylsodium ends (end-biting), or by polymer degradation, when active sites attack through back-biting.^{18,23} The simultaneous formation of lower- and higher-molecular-weight fractions is not well understood so far. It seems that as the degree of polymerization approaches ≈ 50 , the probability of the chain leaving the metal surface increases. This process may be strongly affected by solvent and temperature.²³

Indeed, polar solvents and additives, e.g. crown ethers, cryptands or glymes, increase polymer yields but usually decrease molecular weights.^{14,23,24} Polar solvents appear to promote faster initiation leading to lower molecular weights since more chains form simultaneously, and thus competition for monomers is higher. It is also evident that polar entities solvate $-SiR_2Na$ end groups more efficiently, favoring their departure from the metal surface to the solution. An increase in temperature also facilitates this process.²³

We suggest that the acceleration of the initiation step probably reveals a more efficient e^- -transfer from the metal to the monomer. Besides cation solvation effects, nucleophilic solvents such as THF or glymes can enter into weak donor–acceptor interactions with the halosilane monomer. The strength of these interactions increases with increasing silane acceptor strength. Similar observations were also made with halodisilanes and Lewis bases, and are discussed below. Such donor–acceptor interactions should increase the electrophilicity of



Scheme 3. Competing e^- -transfer between solvated monomers and chain ends (D, donor—solvent, additives).

halosilanes in consequence of an energy lowering of the LUMO.²⁵ This should facilitate e^- -transfer steps. A 'hypercoordinated' monomer accelerating the initiation step is represented in Scheme 3.

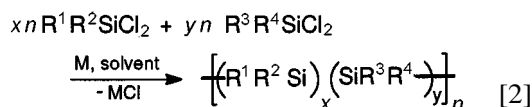
There have been recent efforts to minimize polymodality, to adjust molecular weights and to maximize polymer yields. The best reaction conditions to be indicated so far seem to be preparation at low temperature, use of non-polar solvents and high monomer concentrations.²³

However, the reaction temperature is largely determined by the activation energy of the initiation steps of the reactants. Haloalkylsilanes possess higher reduction potentials than corresponding aryl-substituted monomers. Therefore, for these monomers, temperatures $\geq 80^\circ\text{C}$, sodium as reductant and ultrasonication are needed to initiate polymerization in toluene, while aryl-containing monomers will polymerize at ambient temperature.²³ In the case of dialkyldichlorosilanes, the reaction temperature can be lowered somewhat (60°C) by decreasing oxidation potential of the reductant, using Na–K alloy for example. Crown ether added in traces amounts also decreases the activation energy noticeably, and thus the reaction temperature. The sonochemical preparation method provides an increased active sodium surface due to cavitation erosion, even when polymer preparation is carried out at temperatures below the melting point of sodium (97.5°C). It also accelerates the removal of NaCl from the sodium surface. Besides, sonocation induces selective degradation of preformed high-polymer-weight fractions caused by mechanical shear forces. This leads to nearly monomodal weight distributions and narrow polydispersities.

Further drastic reduction of reaction temperature was achieved by reductive polymerization of dichloromethylphenylsilane in THF with the graphite intercalation compound

C_8K .²⁶ Polymer yields obtained for the reaction carried out at -78°C were between 15 and 23%. The polymer fraction extracted from the graphite phase showed remarkable weight- (\bar{M}_w) or number- (\bar{M}_n) average molecular weights (AMW) of $\bar{M}_w \approx 64\,000$ and $\bar{M}_n \approx 21\,800$, respectively. Interestingly, ^{29}Si NMR spectra reveal an unexpected isotactic content of 50%, assumed to be due to steric constraint being exercised by the lamellar structure of the graphite lattices during chain propagation. However, completely stereoregular polysilylene prepared by reductive coupling has not been reported so far. C_8K -mediated polymerization performed at higher temperatures (between -20 and 25°C) gave low-molecular-weight polymers with a bi- or tri-modal distribution.²⁷ The most important factor determining molecular weights is the C_8K /monomer ratio; an excess of C_8K causes polymer degradation.

Dichlorodialkylsilanes $\text{R}^1\text{R}^2\text{SiCl}_2$ can be copolymerized with other dichlorosilanes $\text{R}^3\text{R}^4\text{SiCl}_2$ containing alkyl or aryl substituents (Eqn [2]).^{14,19}

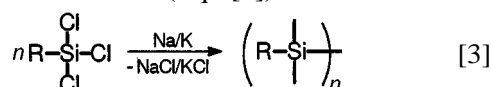


The copolymerization by introduction of different monomer units into the polymer backbone offers a great flexibility in the modification of specific polymer properties, e.g. tractability, solubility, reactivity, glass transition temperature etc.¹⁴ Most of the copolymers show either random or block structures, depending strongly on polymerization kinetics.^{18,19} A higher structural order can be achieved by reductive coupling of α, ω -dihaloorganotrisilanes $\text{ClSiMe}_2\text{R}_2\text{SiMe}_2\text{SiCl}$ ($\text{R} = \text{butyl}$).²⁸ However, the sequence regularity is often altered by competing Si–Si bond cleavage leading to randomization.²⁹

West *et al.* prepared a highly ordered copolymer $(\text{Me}_2\text{Si-Sihex})_n$ (hex=hexyl) by adding Na/K alloy dropwise to a solution of excess $\text{BrSiMe}_2\text{hex}_2\text{SiMe}_2\text{SiBr}$ in refluxing toluene.²⁹ The ^{29}Si NMR spectrum of the low-molecular-weight fraction revealed an alternating sequence of hex_2Si and $(\text{Me}_2\text{Si})_2$ silylene units. However the high-molecular-weight fraction showed partial randomization, indicating enhanced tendency of Si-Si bond cleavage (back-biting) with increasing molecular weight.

2.1.3 Branched polymers

The first branched silicon polymers were reported by Bianconi *et al.*^{30,31} The Si-Si backbones are predominantly constituted by alkylsilylene units $(\text{RSi})_n$ prepared by reductive coupling of trifunctional RSiCl_3 monomers ($\text{R}=\text{CH}_3$, $n\text{-C}_3\text{H}_7$, $n\text{-C}_4\text{H}_9$, $n\text{-C}_6\text{H}_{13}$), using Na/K alloy and ultrasound (Eqn [3]).



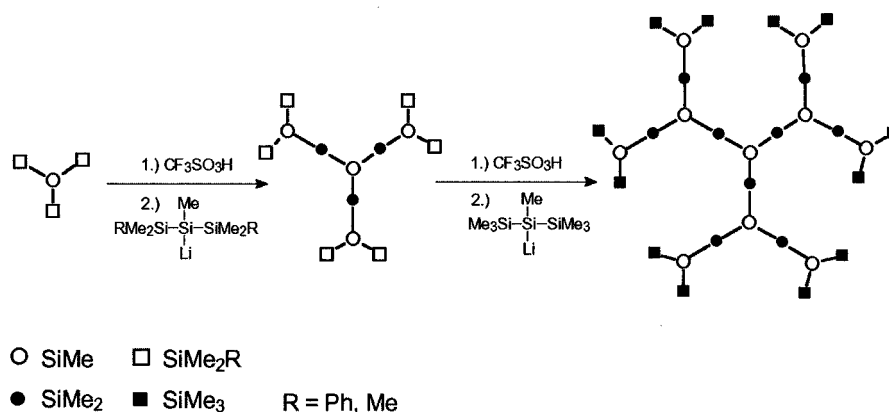
The tetrahedral tertiary silicon backbone sites showed broad overlapping resonance signals in the ^{29}Si NMR spectra between -55 and -58 ppm in solution and between -55 and -65 ppm in the solid state. This clearly indicates the presence of a distribution of silicon entities, related to a backbone of increased rigidity compared with linear polysilylenes. The choice of the alkyl substituents has a major effect on the polymer properties. While poly(methylsilylene) is completely intractable, poly(*n*-hexylsilylene) is extremely soluble in organic solvents. No crystallinity or structural periodicity could be detected by X-ray diffrac-

tion, supporting the presence of a random network built on several conformations: it might be composed of a 2D sheet-like structure or an open cage arrangement of many fused rings. Therefore, polysilynes may represent structural intermediates between polysilylenes and elemental silicon. Matyjaszewski *et al.* suggested that polysilynes resemble dendrimers having 3D rather than flat structures.^{22,32} The formation of a dendritic-like polymer architecture was ascribed to differences in electrophilicity of monomers and polymer end groups, similar to the dehalo-coupling mechanism of dichloro-organosilanes previously mentioned. The architecture becomes hyperbranched and not crosslinked, since the addition of the monomer is kinetically more favored than crosslinking between chains.

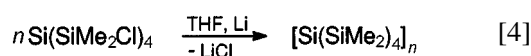
Recently, the synthesis of symmetrical tridentronal polysilane dendrimers was reported, starting from a methylsilylene unit MeSiSi_3 as initiator nucleus.^{33,34} The largest pure starburst-dendrimer known so far was synthesized by successive cycles of protodearylation reactions with triflic acid followed by salt elimination reaction with $\text{RMe}_2\text{SiMeSiLiSiMe}_2\text{R}$ ($\text{R}=\text{Ph}$, Me), as depicted in Scheme 4.³⁴

Recently PhSiCl_3 was homo- as well as copolymerized (PhMeSiCl_2), using C_8K at 20°C in THF.³⁵ However, the as-formed polymers showed a low AMW ($M_w \approx 5000$).

A further increase in the silicon density of the polymer backbone is achieved by incorporation of tetrafunctional monomers, e.g. by means of homopolymerization of tetrakis(halodimethylsilyl)silane, $\text{Si}(\text{SiMe}_2\text{X})_4$ ($\text{X}=\text{Cl}$, Br), which provides dimethylsilylene-bridged *neo*-Si atoms (Eqn [4]).^{22,32}

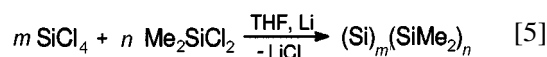


Scheme 4. Synthesis of a dendritic polysilane.



The ^{29}Si NMR spectra of $[\text{Si}(\text{SiMe}_2)_4]_n$ reveal an irregular polymer structure that appears to contain some bicyclic and spiro units. The $\text{Si}(\text{Si})_4$ sites correspond to a broad ^{29}Si NMR signal around -120 ppm, characteristic of a distribution of silicon environments and restricted motion of the polymer backbone as was observed for organosilyne units $\text{RSi}(\text{Si})_3$ in polysilynes.

Another access to polymers containing neo-Si atoms is possible by co-condensing SiCl_4 with di- or tri-functional halo-organosilanes (Eqn [5]).²²



However, the reaction of SiCl_4 with co-monomers is difficult to control, due to favored formation of very oxidation-sensitive silicon clusters.²² Moreover, the reaction with SiCl_4 is often incomplete, providing low yields of soluble materials consisting of a quite high proportion of oligomers.

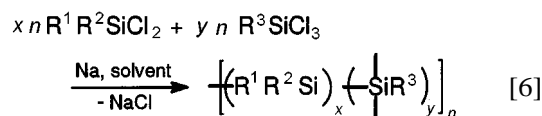
2.1.4 Structure–property relationships

The structure–property relationships of polysilanes will be illustrated by reference to some photophysical properties, indicating the polymer characteristic architecture. The potential of polysilanes as SiC precursors depends not only on their architecture but also on their reactivity.

2.1.4.1 Photophysical properties

The transition from 1D to 2D or 3D polymer architecture drastically changes the opto-electronic polymer properties, such as UV absorption, photoluminescence, fluorescence or photoconductivity. This allows a direct measure of polymer architecture and promises to be a useful tool for adjusting photochemical features by informed control of polymer structure. The introduction of branching in the polymer backbone gives rise to an increase in the spread of Si–Si σ -conjugation as well as a reduction in the band gap energy between the σ HOMO and the σ^* LUMO: the enhanced mobility of σ -electrons therefore causes a decrease in the first ionization potential and in the first optical transition.^{36,36a}

For example, the copolymerization of di- and tri-chlorosilanes leads to polymers showing electronic properties intermediate between polysilylenes and polysilynes (Eqn [6]).^{24,37–39}



The successive introduction of branching in the polymer backbone broadens the absorption/emission spectra and generally shifts the absorption/emission edges to longer wavelength.²⁴ Typical photo-emission of polysilynes is found between 400 and 700 nm.

In comparison, $[\text{Si}(\text{SiMe}_2)_4]_n$ (Eqn [4]) absorbs in the 300 nm region, the typical absorption region for linear polysilylenes, probably caused by SiMe_2 chains that are likely to be formed by redistribution reactions.³² The observed broad and weak emission between 400 and 500 nm suggests that a polymer backbone constituted by isolated quaternary Si atoms each connected by four Me_2Si units is not sufficiently branched to cause the expected strong and long-wavelength emission. In contrast, the introduction of branched organosilyne units by means of copolymerization of $\text{Si}(\text{SiMe}_2\text{Cl})_4$ with PhSiCl_3 shifts the emission to longer wavelengths between 450 and 650 nm.^{22,32}

In the case of $(\text{Si})_m(\text{SiMe}_2)_n$ (Eqn [5]) the luminescence signal broadens and shifts to longer wavelength with an increasing proportion of $\text{Si}(\text{Si})_4$ sites. The emission shift is observed to be the strongest for Me_2SiCl_2 as co-monomer (broad emission between 400 and 500 nm). The influence of $\text{Si}(\text{Si})_4$ sites on emission decreases with the presence of other branching points, derived from RSiCl_3 co-monomers for example.^{22,32}

2.1.4.2 Properties relevant to SiC fiber precursors

Polysilyne-related copolymers can be used as SiC precursors, mainly because of improved ceramic yields compared with those obtained with linear polysilylenes.^{40,41} In this context Sharp and co-workers have synthesized several copolysilanes with different proportions of branching units and various organic side groups according to Eqn [6] ($\text{R}^1 = \text{CH}_3$, C_6H_5 ; $\text{R}^2 = \text{CH}_3$, C_6H_5 ; $\text{R}^3 = \text{C}_6\text{H}_5$, C_2H_5).⁴² The best ceramic yields were obtained for copolymers derived from PhSiCl_3 and Me_2SiCl_2 , ranging from 69 to 84% depending on the proportion of monomer in the starting mixture. The free carbon contents are not reported; however they are likely to increase with an increase in the C/Si ratio in the starting polymers. Moreover, some of these polymers

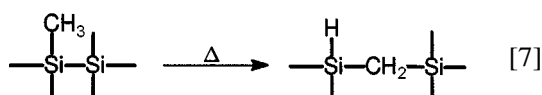
were successfully melt-spun, demonstrating that even branched polymers can be processed readily to continuous polymer fibers. However, the spinnability varies considerably and seems to be strongly affected by organic substituents. Generally the introduction of phenyl groups improves polymer spinnability. On the other hand, unfavorably high C/Si ratios result.

Currently it is rather difficult to define clearly rules for spinning of organosilicon polymers. One reason might be a lack of comparable published results. The understanding of the relationships between organosilicon polymer architecture and the corresponding rheological behavior, essential for spinning, is just in its infancy. Rheological models developed for pure organic polymers have to be adapted when applied to organosilicon polymers.⁴³

Polymer spinnability is only one important polymer feature necessary for SiC fiber manufacture. Once spun, the polymer fibers (generally collected on a reel) should not be brittle, because they have to be unwound subsequently from the reel for further continuous pyrolysis. Moreover, to prevent fiber distortion during pyrolysis, the pre-ceramic fiber has to be unmeltable. This is achieved either by dry spinning (from solution) of soluble but non-fusible polymer fractions⁴⁴ or by crosslinking of melt-spun polymer fibers (curing). The latter step, however, requires a certain level of latent polymer reactivity.

2.1.4.3 Polymer reactivity

As already mentioned, quantitative reductive dehalogenation of the starting monomers gives rise to low latent reactivity. For example, poly-(dimethylsilane) (PDMS) derived from dehalocoupling of Me_2SiCl_2 , is intractable and thus cannot be spun readily into fibers. Most of the polymer is removed as volatile species during pyrolysis due to its low capability to undergo crosslinking reactions. Consequently very low ceramic yields result. These drawbacks are partially overcome by thermal pretreatment of PDMS to 430–470 °C, where the polysilylene backbone undergoes skeletal ‘Kumada’ rearrangement to form polycarbosilane (PCS) $[\text{MeHSiCH}_2]_x$.⁴⁵



The reaction mechanism was assumed to involve radical steps.⁴⁶ Recently it was suggested that

silylene or silene intermediates form, because they have been observed in the gas phase during pyrolysis of permethylated oligosilanes.⁴⁷ Although the PCS is rather oligomeric ($\bar{M}_n=1200\text{--}2000$) it can be spun from melt. The as-introduced reactive Si—H bonds are essential for the curing of the polymer fiber, which is mainly performed by reaction with oxygen leading to Si—O—Si crosslinking.⁴⁸

Pyrolysis of poly(hydro-organosilanes) $[\text{RHSi}]_x$, synthesized by dehalocoupling of Si—H containing monomers,¹⁹ has also shown that Si—H backbone functionalities have a beneficial effect on crosslinking during pyrolysis. Thus decomposition is retarded and ceramic yields increase.⁴¹

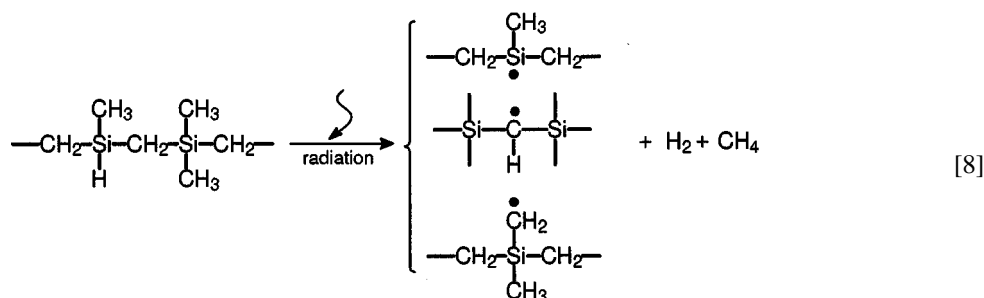
In general radiation-initiated reactions also introduced pre-ceramic fiber curing. The sensitivity of Si—Si or Si—C bonds radiation depends on the irradiation wavelength. The relatively weak Si—Si bonds can be cleaved by photolysis, producing reactive silyl radicals and silylenes.⁴⁹ Therefore polysilanes can also be used as photoinitiators in vinyl polymerization⁵⁰ or are employed as UV-acting photoresists (polysilane crosslinking or degradation), e.g. in micro-lithography.^{20,51–53}

PCS fibers can be cured by irradiation with γ -ray or electron beam.^{54–61} The high-energy radiation cleaves Si—C and Si—H as well as C—H bonds homolytically, generating silicon and carbon radicals on the PCS main chain. Finally, radical combination reactions take place leading to crosslinking and evolution of hydrogen and methane (Eqn [8]). Indeed, the pyrolysis of PCS fibers irradiated in helium provides SiC fibers with oxygen contents lower than 0.4 wt%.

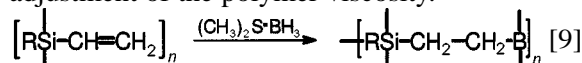
2.1.4. Chemical modification

It has been proved that the Si—H monomer functionalities can only be partly retained during dehalocoupling because they undergo uncontrolled side reactions leading to branching and crosslinking.^{62,63} Seyferth *et al.* have used remaining Si—H functionalities to crosslink poly-(methylsilane) $[(\text{MeSiH})_x(\text{MeSi})_{1-x}]$ (PMS) by hydrosilylation with organic or organosilicon compounds in order to increase both the ceramic yield on pyrolysis and the C content of PMS.⁶⁴ PMS was originally synthesized upon dehalocoupling of MeHSiCl_2 with sodium.⁶⁵

The preservation of Si—Vi (Vi=vinyl) groups succeeds in sodium-promoted co-condensation of $\text{Me}_x\text{SiCl}_{4-x}$ ($x=1, 2, 3$) and $\text{Me}(\text{CH}_2=$



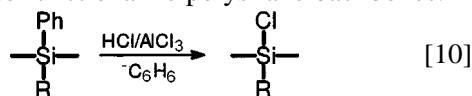
CH)SiCl₂ in THF.^{40,62,63} In such a way vinylic copolymers and terpolymers were obtained. Additionally, MeHSiCl₂ may be applied instead of Me₂SiCl₂, thus aiding the increase of ceramic yields on pyrolysis. The use of reductants of lower oxidation potential, such as potassium, gives rise to silylation of vinyl groups, losing the reactive centers on the polymer backbone. Vinylic substituents offer further opportunities for modification, such as hydrosilylation^{66–68} or hydroboration (Eqn [9]),⁶⁹ providing a means of controllable polymer crosslinking and thus adjustment of the polymer viscosity.



Hydroboration crosslinking is a promising method for production Si–C–B fibers of low oxygen content. The boron which is incorporated increases ceramic yields on pyrolysis as well. Low boron contents (>2 wt%) improve the sinteractivity of SiC.

The stimulation of the polymer reactivity can be also achieved by electrophilic or nucleophilic substitution of organic side groups involving Si–C bond cleavage. The latter should occur without significant backbone destruction. However, due to the highly delocalized σ backbone of polysilanes, a low oxidation potential results.⁷⁰ The positive charge of polysilane radical cations can largely delocalize over the Si–Si skeleton. This is in good agreement with the small ionization energies measured by photoelectron spectroscopy (<10 eV).⁷¹ This redox behavior limits the use of strong electrophiles for substitution reactions. However, strong nucleophiles can also give rise to Si–Si backbone degradation.

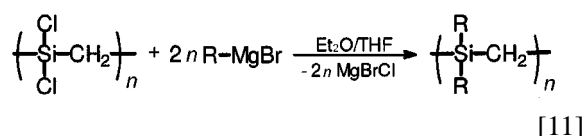
So far, the substitution of phenyl groups by HCl/AlCl₃ treatment (Eqn [10]) is the preferred method to functionalize polysilane backbones.¹⁹



The phenyl substitution also succeeds for several phenyl-containing copolysilenes, poly(silylene-co-alkylene)s or poly(carbosilane)s.^{72,73} A similar approach was followed for the AlCl₃-catalyzed interchange reaction of chlorine and methyl groups using Me₃SiCl as chlorine donor, in the case of oligosilanes, polysilanes and even poly(carbosilane)s.^{74,75}

Si–C bonds may also be cleaved using HCl/AlCl₃, MeCOCl/AlCl₃, SO₂Cl₂ or NH₄Cl/H₂SO₄ treatments.^{21,76,77} However, these methods mainly provide a way of introducing Si–Cl bonds on the terminal silyl groups of oligomers.

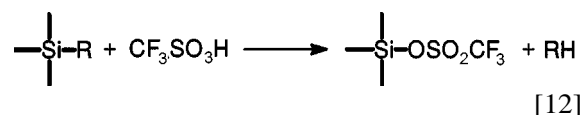
The Si–Cl functionalities generally offer a wide variety of further possible polymer modifications by reaction with nucleophiles, which will not be extensively discussed in this review.^{21,75} For example, Sartori and co-workers have recently synthesized dialkenyl or dialkynyl-substituted poly(silylene-co-methylene)s upon alkenylation (R=CH=CH₂, CH₂CH=CH₂, CH₂C(CH₃)CH=CH₂...) or alkynylation [R=C≡CH, C≡C(CH₂)₂CH₃...] of poly(dichlorosilylene-co-methylene)s via Grignard reaction:⁷⁹



The ethynyl derivatives may be more specifically suited for SiC fiber applications. They can be melt-spun easily to continuous polymer fibers.^{80,81} The ethynyl groups allow sufficient cross-linking of the pre-ceramic fibers by UV irradiation. The fibers obtained after pyrolysis showed a good thermal stability in argon for $T \leq 1700$ °C.

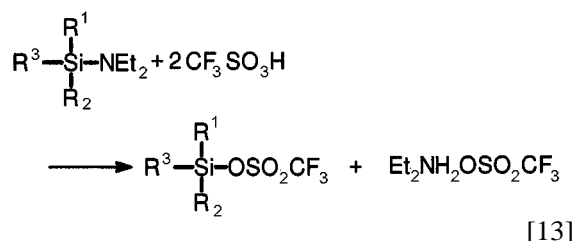
Another promising functionalization reagent is trifluoromethanesulfonic (triflic) acid.^{16,82} Silyl triflate polymer derivatives are formed upon protodesilylation with triflic acid, mainly for

R=phenyl, benzyl and allyl (Eqn [12]) or aminosilyl groups bonded to organosilicon polymer backbones (Eqn [13]).^{16, 83, 84}



The tendency of Si–R bond cleavage decreases in the order allyl > α -naphthyl > phenyl > Cl, vinyl, $\text{OC}_n\text{H}_{n+2}$ > H \gg alkyl.^{83, 85} This allows selective substitution of different organic groups. In this way, polysilanes, poly(silylene-co-alkyne)s, poly(silylene-co-arylidene)s or poly(carbosilane)s have been recently modified.^{84, 86–88}

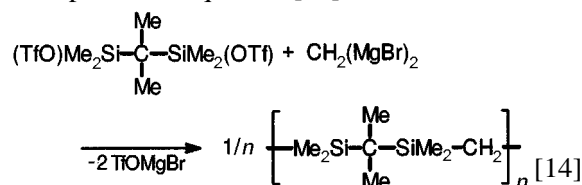
The silyl triflates react with nucleophiles under mild conditions, providing high yields and short reaction times.⁸⁹ It has been shown that diethylamino groups are substituted preferentially compared with organic ones:



This makes their use as protecting groups in monomer or polymer synthesis of great interest ($\text{R}^{1,2,3} = \text{Me}$, allyl, vinyl, Ph, Cl, H, OMe, Et₂N).⁹⁰ Scheme 5 provides a brief outline of possible

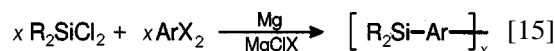
chemical modifications of polysilanes and poly(carbosilane)s and related copolymers.

Triflate-disubstituted organosilanes may also be coupled upon salt elimination, producing well-defined poly(carbosilane)s and related copolymers with a regular alternating arrangement of silylene and organic monomer units, e.g. as depicted in Equation [14].⁸⁸



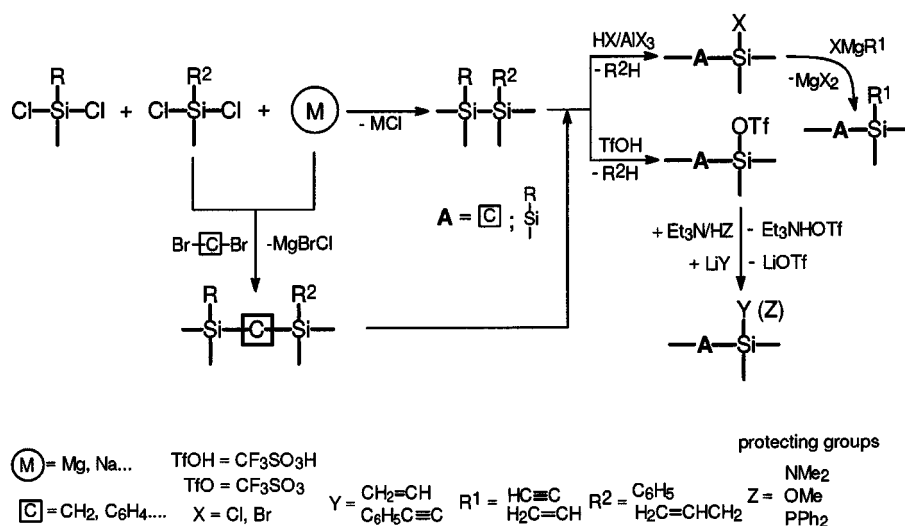
The sharp signals in the ²⁹Si and ¹³C NMR spectra may indicate that the condensation is not accompanied by randomization.

In a similar synthesis, the Grignard-coupling of R_2SiCl_2 [$\text{R}_2 = \text{Me}$, H; Me, Vi (vinyl); Vi_2 ; All_2 (allyl) ...; Me, $(\text{C}\equiv\text{C}(\text{CH}_2)_x\text{CH}_3)$, $x = 2-4$; $(\text{C}\equiv\text{C}(\text{CH}_2)_x\text{CH}_3)_2$] and ArX_2 ($\text{Ar} = \text{CHC}_6\text{H}_5$, $p\text{-C}_6\text{H}_4$...; $\text{X} = \text{Br}$, Cl) provides multicarbon-bridged silylene units. The as-formed polymers are oligomeric rather than polymeric. The reactive functionalities can be completely retained in the course of the reaction:⁹¹



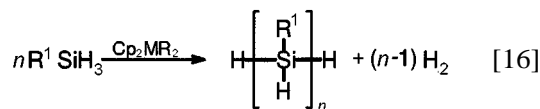
2.2 Catalytic dehydropolymerization

Harrod's discovery that H-functional monosilanes can be linked by formation of Si–Si



Scheme 5. Introduction of reactive substituents in polysilane and poly(carbosilane) backbones.

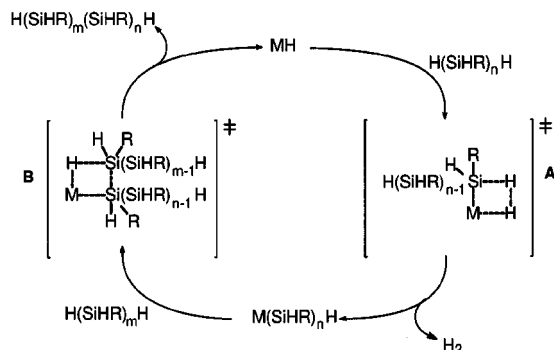
bonds in the coordination sphere of transition-metal complexes ($M = \text{Ti, Zr}$; $R = \text{Me, PhCH}_2$; $R^1 = \text{Ph, Hex}$) offers access to H-containing (and thus reactive), but low-molecular-weight, polysilanes.^{7,92}



The reaction mechanism seems to be a step-growth mechanism that is based on a disproportionation of $\sigma\text{-Si-H}$ to Si-Si and H-H bonds.⁸ Tilley has postulated a σ -bond metathesis mechanism involving four-center transition states in which σ -bonds are broken and formed (Scheme 6).^{8,93} $M\text{-H}$ represents the coordinatively unsaturated metal hydride which acts as the active catalyst (d^0 metal hydride). The proposed mechanism is based on two steps: the dehydrometalation of the silane with the metal hydride (**A**) and the coupling of the metal silyl complex with the hydrosilane resulting in Si-Si bond formation (**B**).

Further investigations have shown that molecular weights and the proportion of cyclic oligomers formed depend strongly on the catalyst applied and the reaction temperature as well as on the nature of R^1 .⁹⁴ Recently, it has been reported that a neodymium catalyst Cp^*_2NdR [$Cp^* = \eta^5\text{-C}_5\text{Me}_5$; $R = \text{CH}(\text{SiMe}_3)_2$] promotes dehydropolymerization of PhSiH_3 (80 °C, autoclave) giving a polysilane with an AWM of $\bar{M}_w \approx 780$. The polymer structure is suggested to be mainly cyclic. A higher AWM ($\bar{M}_w \approx 1600$) can be obtained at elevated reaction temperatures (130 °C) or on thermal treatment (160 °C, $\bar{M}_w \approx 4830$), indicating that the catalyst still remains active.

In general the Si-H functionalities provide a



Scheme 6. σ -bond metathesis mechanism.

further possibility of crosslinking upon thermal treatment in the presence of the catalyst. However, thermal treatments do not always lead to higher molecular weights. Instead, degradation of linear chains can occur forming mainly thermodynamically stable cyclics, as observed for $[\text{PhSiH}]_x$ with $\text{CpCp}^*\text{Zr}[\text{Si}(\text{SiMe}_3)_3]\text{Me}$ as catalyst.⁸

According to Eqn [16], poly(methylsilane) $[\text{MeSiH}]_x$ can be derived from MeSiH_3 in toluene using Cp_2MMe_2 ($M = \text{Zr, Ti}$) as catalyst. Laine and co-workers reported values of $\bar{M}_w \approx 10\,000$ to $12\,000$ and $\bar{M}_n \approx 1200$ with less than 3% cyclics.⁹ $[\text{MeSiH}]_x$ can be spun directly from the cyclohexane reaction solution, if the polymerization is performed in presence of cyclohexene.⁵ However, the polymer fibers melt on pyrolysis unless the polymer is modified (to achieve higher molecular weights) or mixed with higher-molecular-weight fractions. Therefore Laine and colleagues have modified the oligomeric $[\text{MeSiH}]_x$ producing a star-branched polymer of higher molecular weight, that may display an excellent spinnability (Fig. 1).

Recently Seyferth *et al.* have used Group 4 metallocene catalysts [$(\eta^5\text{-C}_5\text{H}_5)_2\text{ZrH}_2$, $(\eta^5\text{-C}_5\text{H}_5)_2\text{ZrHCl}$] to crosslink poly(vinylsilane), PVSih_3 .⁹⁵ PVSih_3 was derived from ^{60}Co γ -radiation-induced polymerization of $\text{CH}_2=\text{CHSiCl}_3$ and subsequent LiAlH_4 reduction of the $-\text{SiCl}_3$ groups.^{95,96} The crosslinking of PVSih_3 via metallocene catalysts improved the ceramic yield on pyrolysis (1500 °C) from 40%

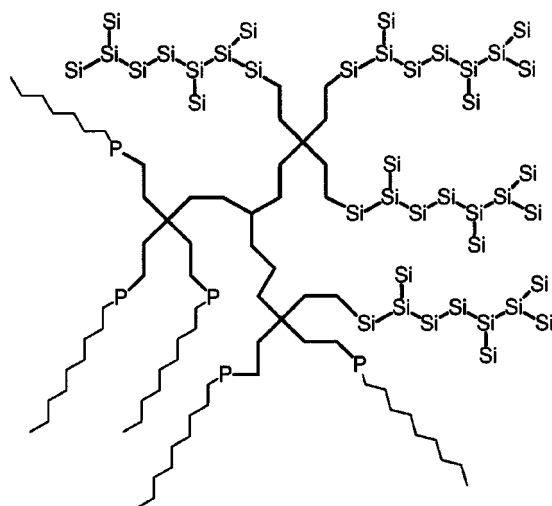


Figure 1. Star-branched poly(methylsilane); P represents a PMS oligomer 10 Si units long.⁵

to 70–80 wt%. The ceramic residue contained 10–13 wt% of carbon.

Dehydropolymerization of methylidisilanes such as $\text{MeH}_2\text{Si}-\text{SiH}_2\text{Me}$ in the coordination sphere of titanium or zirconium cyclopentadienyl complexes^{10–12} gives predominantly branched polysilane backbones based on tertiary Si atoms, $\text{R}-\text{Si}(\text{Si})_3$ (Eqn [17]). The oligomers were detected during the first stage of the reaction, which is difficult to control because of the permanent presence of the catalyst. Hengge postulated a mechanism involving silylene intermediates formed by cleavage of a transition-metal silylene complex $\text{L}_2\text{M}=\text{SiMe}_2$. Such a mechanism has been reported for the oligomerization of $\text{Me}_3\text{Si}-\text{SiMe}_2\text{H}$ leading to linear oligomers and the monosilane Me_3SiH ^{10,12} (Scheme 7). This complex is supposed to be formed through the so-called β^* -bond elimination from a four-center transition state. The Si–Si bond cleavage is the decisive step in the formation of oligosilane backbones. The silylenes obviously extend the silicon backbone by insertion in both functional bonds, Si–H and Si–Si.

In the case of $\text{MeH}_2\text{Si}-\text{SiH}_2\text{Me}$ polymerization, the existence of linear as well as branched

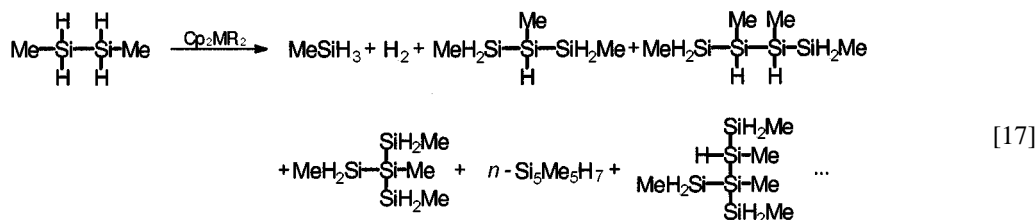
oligosilanes and moreover of H_2 in addition to MeSiH_3 as gaseous products, suggests the overlap of two different polymerization mechanisms. The insertion of silylenes into Si–H bonds may lead mainly to branched oligomers. The formation of quaternary silicon backbone atoms $\text{Si}(\text{Si})_4$ is prevented since silylenes do not insert in Si–C bonds. The additional H_2 formation seems to be caused by σ -bond metathesis which forms linear oligosilanes or couples oligomers to each other. Finally, in the late stage of the reaction, cross-linking takes place leading to an insoluble and infusible polymer of a type unknown so far, with a general composition $(\text{SiMeH}_{0.58})$.^{10,11} The polymer gives a high ceramic yield on pyrolysis, of about 88%.¹⁰

2.3 Catalytic disproportionation of halodisilanes

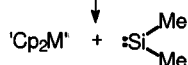
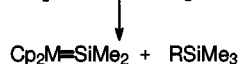
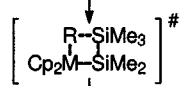
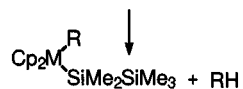
2.3.1 Basic routes to chloromethyloligosilanes

If the H-substituents of disilanes are replaced by chlorine, as in $\text{MeCl}_2\text{Si}-\text{SiCl}_2\text{Me}$ (**2**), the disilanes can be converted into oligo- or polysilanes by a Lewis-base (**D**)-catalyzed disproportionation (Eqn [18]).

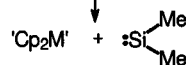
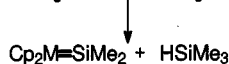
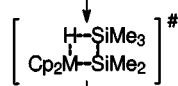
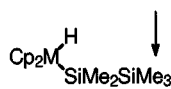
The starting tetrachlorodimethyldisilane **2** can



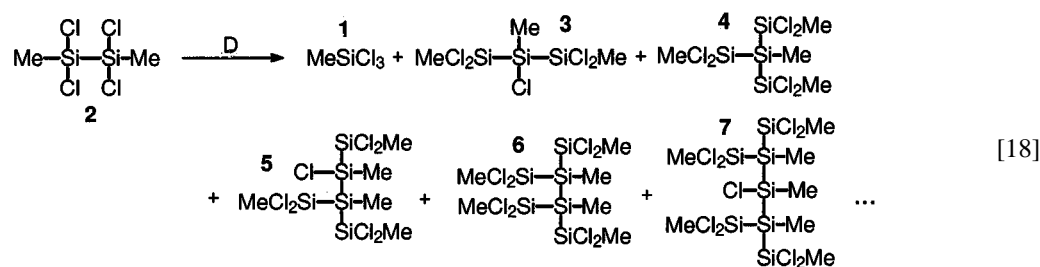
Formation of the active catalyst



Polymerisation



Scheme 7. Proposed β^* -elimination mechanism of the dehydropolymerization of $\text{Me}_3\text{Si}-\text{SiHMe}_2$.



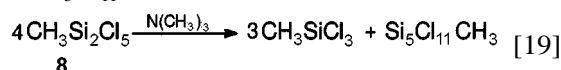
be obtained easily^{76,77} from a mixture of several chloromethyldisilanes $\text{Me}_x\text{Cl}_{6-x}\text{Si}_2$ ($x=1-5$), which are by-products of the industrial 'Direct Synthesis' (Müller-Rochow) of chloromethylmonosilanes, precursors for silicone products.

Recently we reported the ^1H , ^{29}Si , ^{13}C NMR and GC-MS identification of the chloromethyloligosilanes **3**, **4**, **5**, **6** and **7** formed in the early stages of the reaction.⁹⁷ The monosilane MeSiCl_3 (**1**) can be removed easily by distillation from the oligosilane mixture. The ^{29}Si NMR spectrum of such a mixture is shown in Fig. 2 and the ^{29}Si and ^{13}C NMR chemical shifts of the oligomers are summarized in Table 1.

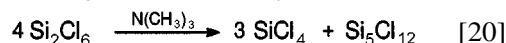
Surprisingly, as depicted in Eqn [18], oligosilane backbones such as the trisilanes and the higher branched oligosilanes similar to those obtained through dehydropolymerization of $\text{MeH}_2\text{Si}-\text{SiH}_2\text{Me}$ (Eqn [17]) are obtained. Linear oligomers with Si_n ($n>3$) have never been observed, nor have branched oligomers higher than the isoheptasilane **7** or other constitutional

isomers.

Trandell and Urry disproportionated the disilanes $\text{MeCl}_2\text{Si}-\text{SiCl}_2\text{Me}$ **2**, $\text{MeCl}_2\text{Si}-\text{SiCl}_3$ **8** and Si_2Cl_6 **9**.⁹⁸ In the case of **2**, they obtained the isotetrasilane **4** as the dominant species besides the monosilane MeSiCl_3 **1** using trimethylamine as catalyst (17 d, 65°C). The disproportionation of **8** induced by $\text{N}(\text{CH}_3)_3$ (24 h, 20°C) gave pure neo- $\text{Si}_5\text{Cl}_{11}\text{Me}$ after sublimation:



$\text{N}(\text{CH}_3)_3$ forms a very unstable adduct with **9** at temperatures below -78°C . The disilane disproportionation is immediately induced by increasing the temperature, giving quantitatively SiCl_4 , neo- $\text{Si}_5\text{Cl}_{12}$ and neo- $\text{Si}_6\text{Cl}_{14}$.^{99,100}



Recently we succeeded in the disproportiona-

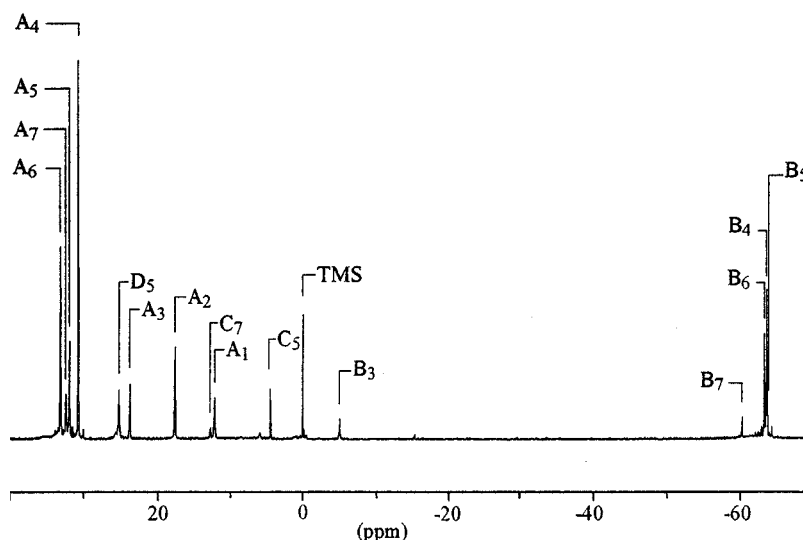
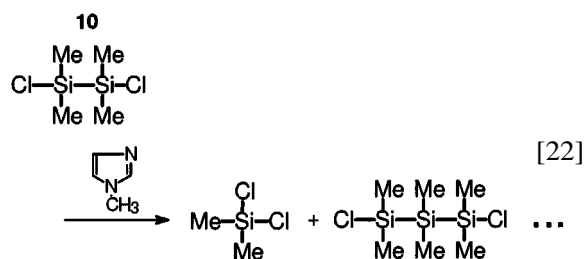


Figure 2 ^{29}Si NMR spectrum of the chloromethyloligosilanes **1-7** (X_n refers to the Si^x site in silane n whose chemical shift is reported in Table 1).

Table 1 ^{29}Si and ^{13}C NMR chemical shifts of the chloromethyloligosilanes **1–7**

Silane	Formula	$\delta^{29}\text{Si}$ (ppm)		$\delta^{13}\text{C}$ (ppm)
1	MeSiCl_3	12.2		9.69
2	$\text{MeCl}_2\text{Si}-\text{SiCl}_2\text{Me}$	17.6		4.95
3	$(\text{MeCl}_2\text{Si}^{\text{A}})_2\text{Si}^{\text{B}}\text{ClMe}$	23.8	A	6.50
		−4.9	B	−2.70
4	$(\text{MeCl}_2\text{Si}^{\text{A}})_3\text{Si}^{\text{B}}\text{Me}$	30.7	A	9.01
		−63.5	B	−12.62
5	$(\text{MeCl}_2\text{Si}^{\text{A}})_2\text{Si}^{\text{B}}\text{Me}(\text{Si}^{\text{C}}\text{ClMe})\text{Si}^{\text{D}}\text{Cl}_2\text{Me}$	32.1	A	9.44
		−63.7	B	−11.87
		4.4	C	0.52
		25.2	D	6.58
6	$[(\text{MeCl}_2\text{Si}^{\text{A}})_2\text{Si}^{\text{B}}\text{Me}]_2$	33.1	A	9.68
		−63.2	B	−10.04
7	$[(\text{MeCl}_2\text{Si}^{\text{A}})_2\text{Si}^{\text{B}}\text{Me}]_2\text{Si}^{\text{C}}\text{ClMe}$	32.4	A	9.62
		−60.2	B	−10.98
		12.8	C	4.25

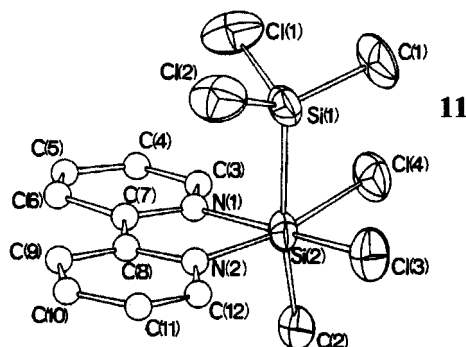
tion of $\text{Me}_2\text{ClSi}-\text{SiClMe}_2$ (**10**) with *N*-methylimidazole as catalyst, a reaction which had not been observed so far. The reaction gave α,ω -dichloro-oligosilane chains as well as the monosilane Me_2SiCl_2 (Eqn [22]).⁹⁷

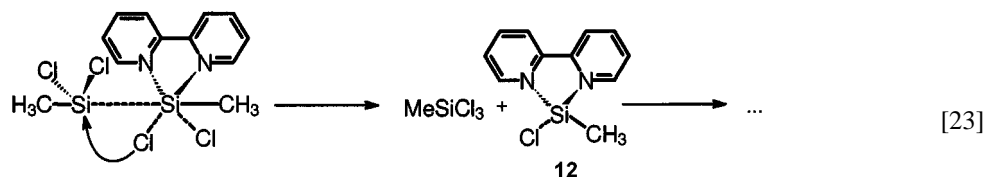


The result is also in agreement with that found for the dehydropolymerization of $\text{Me}_2\text{HSi}-\text{SiHMe}_2$.¹¹

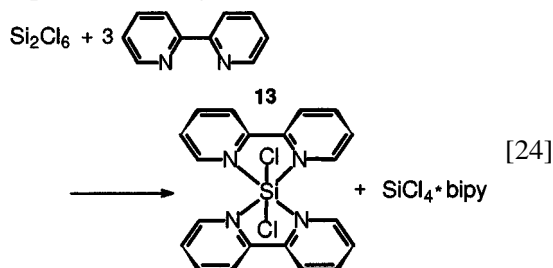
The disproportionation mechanism of halodisilanes is largely unknown. Generally disilanes undergo Si–Si bond cleavage by nucleophilic attack of Lewis bases. Nevertheless, Kummer *et al.* succeeded in isolating some adducts between bidentate ligands such as bipyridyl (bipy) or 1,10-phenanthroline (phen) with Si_2Cl_6 , $\text{Si}_2\text{Cl}_3\text{Me}_3$ or Si_3Cl_8 , for example.¹⁰¹ According to these investigations the 1:1 adduct **11** between **2** and bipy (Fig. 3) is formed exclusively, obviously due to steric effects. The crystal structure of **11**¹⁰² shows that both N-donor atoms are coordinated to the same silicon atom of **2**. The sterically demanding ligands $-\text{SiCl}_2\text{Me}$ and $-\text{CH}_3$ are arranged vertically with respect to the plane of the bipy ligand. The less demanding Cl

atoms are situated in the equatorial position. A characteristic feature of adduct **11** is that both Si–Cl bonds are unusually long (average 233 pm): this allows the assumption that the starting point of the disproportionation of halodisilanes is an ionization of covalent Si–Cl bonds and a subsequent cleavage of the Si–Si bond (Eqn [23]). Indeed, the complex decomposes in polar solvents such as THF at 25 °C, turning green. As a result of the decomposition, the Lewis-base-stabilized chloromethylsilylene intermediate **12** will certainly be generated. However, it has not been possible to prove the formation of **12** so far. Instead, around 150 °C the formation of oligomers as well as of the monosilane MeSiCl_3 has been confirmed experimentally but the oligomers were not identified.¹⁰³ In contrast, evidence for silylene intermediates has been successfully obtained in the reaction between Si_2Cl_6 and bipy:

**Figure 3** ORTEP diagram of the $\text{Si}_2\text{Cl}_4\text{Me}_2 \cdot \text{bipy}$ adduct **11**.¹⁰²



using a bipy/ Si_2Cl_6 molar ratio of 3 (25 °C, THF), the formation of the dichlorosilylene complex **13** (dark green) has been observed.¹⁰⁴



Kummer suggested that the silylene formation is caused by an α -elimination.¹⁰⁴ Moreover, complexes formed from methyl-rich disilanes such as $\text{Me}_2\text{ClSi}-\text{SiCl}_2\text{Me}$ and bipy or phen are only stable at temperatures below -80 °C. These facts indicate a decrease in acceptor strength when the number of bonded methyl groups per silicon increases. Taking into account the decreasing stability of the bipy complexes in the order $\text{Si}_3\text{Cl}_8 > \text{Si}_2\text{Cl}_6 > \text{MeCl}_2\text{Si}-\text{SiCl}_2\text{Me} > \text{Me}_2\text{ClSi}-\text{SiCl}_2\text{Me}$, it was concluded that the silyl substituents considerably increase the acceptor strength of the α -Si atom of the disilane in the order $\text{SiMe}_3 < \text{SiClMe}_2 < \text{SiCl}_2\text{Me} < \text{SiCl}_3$. The effect of Cl is comparable with that of the SiMe_3 group.¹⁰¹ In fact a strong indication of this was found in the structure of $\text{Si}_3\text{Cl}_8 \cdot \text{phen}$, **14** (Fig. 4), in which the phen ligand is coordinated to the central Si atom:¹⁰⁵ the electron-withdrawing effect of each of the three chlorine substituents is overcome by the two silyl groups.

2.4. Novel synthetic procedures

Previously applied catalysts are electron-pair donors such as amines,^{98,106,107} quaternary ammonium^{106–108} or phosphonium salts (Cl^-),¹⁰⁶ AgCN ¹⁰⁹ or hexamethylphosphoric triamide^{110,111} which were added to the disilanes in catalytically effective amounts of about 0.5–5 wt%. As already mentioned for the dehydropolymerization, the formation of chloromethyloligosilanes can only be controlled with difficulty due to the

permanent presence of the catalyst, even considering that the reactivity of chloromethyloligosilanes is comparatively weaker than for H-containing oligosilane mixtures with titanocene or zirconocene catalysts. For structural studies as well as for the application of these polymers, it is advantageous to stop the polymerization at a certain stage of the reaction and to be able to separate the catalyst from the parent compounds and reaction products. Therefore we grafted effective catalytic centers such as bis(dimethylamido)phosphoryl (**15**), benzimidazolyl (**16**) or 3,5-dimethylpyrazolyl (**17**) groups onto the surface of silica carriers **18**, using organotrialkoxysilane spacers as graft mediators (Eqn [25]).^{112,113}

It has been proved that on average 2.3 alkoxy groups react with OH groups of the silica surface (**18**). The catalyst grains can be stored in a reactor. The vaporized disilanes (e.g. $\text{MeCl}_2\text{Si}-\text{SiCl}_2\text{Me}$ has a b.p. of 154 °C) are carried in an argon stream to the catalyst bed. The reaction starts on the catalyst surface. The as-formed monosilanes and oligosilanes are removed from the catalyst. In such a manner $\text{MeCl}_2\text{Si}-\text{SiCl}_2\text{Me}$, $\text{Me}_2\text{ClSi}-\text{SiCl}_2\text{Me}$ or $\text{Me}_3\text{Si}-\text{SiCl}_3$ can be disproportionated. The disproportionation is not observed for the methyl-rich disilanes $\text{Me}_2\text{ClSi}-$

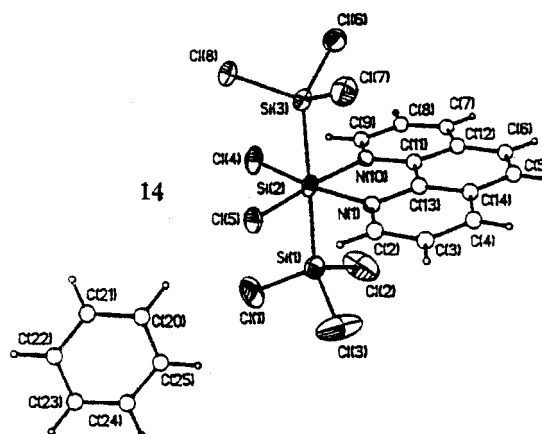
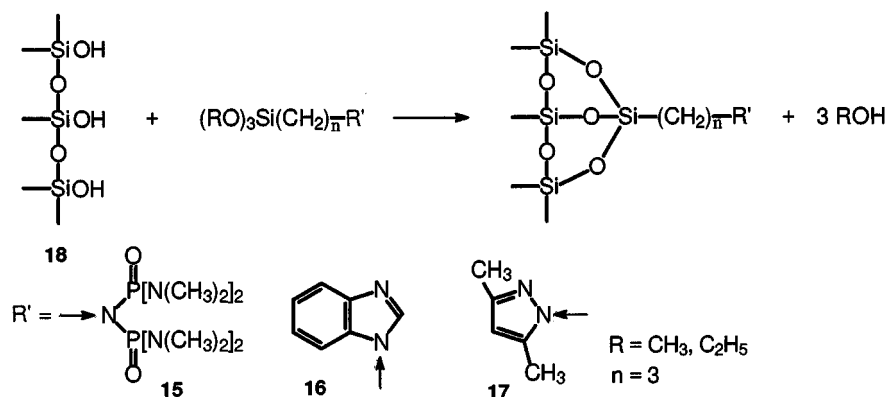


Figure 4 Perspective view of the $\text{Si}_3\text{Cl}_8 \cdot \text{phen} \cdot \text{C}_6\text{H}_6$ adduct **14**.¹⁰⁵



SiClMe_2 or $\text{Me}_3\text{Si-SiClMe}_2$, due to their lower acceptor strength.

2.5 Mechanism of the disproportionation of chloromethyldisilanes

Our investigations on the disproportionation of **2** have shown that the trisilane **3** and the isotetrasilane **4** are formed directly on the catalyst surface. These observations lead to the following conclusions. The essential catalytic step is the reversible nucleophilic attack of the electron-pair donor (N, P=O or $\text{N}(\text{CH}_3)_2$) leading to the formation of a pentacoordinated Si atom in the disilane molecule as depicted in Scheme 8.¹¹⁴ The kinetics of the complex formation and its

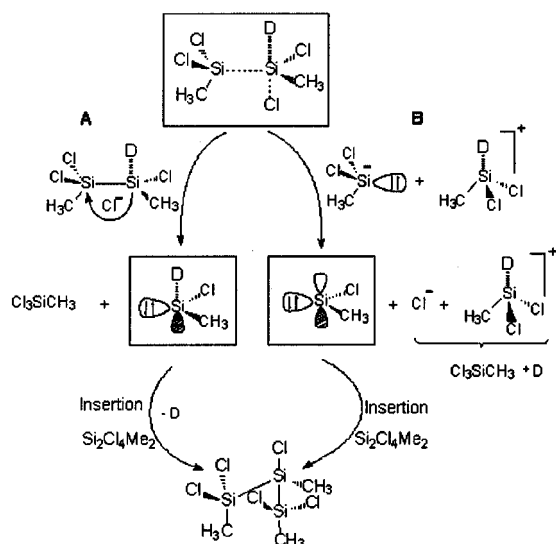
stability are primarily governed by the nucleophilicity of the Lewis base, the steric conditions and the acceptor strength of the halosilanes.

The electron-donor capability of the Lewis base should be correlated with the value of the first ionization potential of the electron-pair donor: the lower the ionization potential, the higher the electron-donor capability is expected to be. We found that Lewis bases with first ionization energies smaller than 9 eV are effective catalysts for the disproportionation of halosilanes. The values of the first ionization energies for some nitrogen-containing catalysts are shown in Table 2.^{115, 116}

We performed *ab-initio* quantum-chemical calculations to gain a better insight into the mechanism proposed in Scheme 8. The molecules investigated are summarized in Table 3 with their total energies and HOMO/LUMO energies. We considered $\text{O}=\text{PH}_3$ as a model compound for the base derived from the bis(dimethylamido)phosphoryl catalyst that we have mainly used for the catalytic disproportionation of halosilanes. According to the difference between the total energies, the formation of the adduct **19** (Fig. 5) between $\text{Cl}_2\text{MeSi-SiMeCl}_2$ and $\text{O}=\text{PH}_3$ is exothermic (87.4 kJ mol^{-1}). The extension of the coordination sphere of the originally tetracoordinated Si atom lowers the LUMO energy from 3.01 eV in **2** to 2.88 eV in **19**. This effect causes an increase in the electrophilicity of the molecule.²⁵

Nevertheless, there is no information about the transition states of these reactions, and moreover the calculations neglect solvent or surface effects. These are the usual drawbacks of quantum-chemical calculations.¹¹⁷

The optimized structure of **19** (Fig. 5) shows some interesting features. Whereas three Si-Cl



Scheme 8. Proposed disproportionation mechanism of $\text{MeCl}_2\text{Si-SiCl}_2\text{Me}$ (**2**).

Table 2 First ionization potentials of nitrogen-containing compounds^a

Compound	First ionization energy (eV)
1-Ethyl-3,5-dimethylpyrazole	8.41
1-Ethylbenzimidazole	8.16
1-Methylimidazole	8.69
Hexamethylphosphoric triamide	8.10

^a For simplification, one alkyl or dimethylamino group substitutes the silylalkylene spacer unit bonded to the silica carrier.

bonds have normal lengths between 2.041 and 2.079 Å, one Si–Cl bond is extremely long (3.137 Å). The sum of the covalent radii of silicon and chlorine is 2.16 Å, and the sum of the van der Waals radii is 3.9 Å. The calculated distance of 3.137 Å is between these values, indicating that this chlorine atom is on the way to leaving the molecule due to the coordination effect on the model base. The coordination sphere of the silicon atom Si1 has a distorted pentagonal bipyramidal geometry with the chlorine atoms located in axial positions. The coordination geometry of Si2 is tetrahedral.

As a result of the Si–Cl bond ionization, the chloride ion migrates to the tetrahedral silicon atom of **20** as shown in Scheme 8. The chloride transfer can also succeed with formation of μ_2 -chloro bridges. The formation of the thermodynamically stable monosilane MeSiCl₃ should lead finally to Si–Si bond cleavage, leaving a donor-stabilized chloromethylsilylene on the catalyst surface. Path **A** can thus be described as an α -elimination step. Chloride ions can also exert a catalytic effect upon Si–Si bond cleavage on the catalyst surface, since chloride is able to act itself as an electron-pair donor.

Alternatively one can take into account the reaction path **B**, in which the Si–Si bond cleavage proceeds with the formation of a silanion and a donor-stabilized silicenium ion.

The two reaction pathways **A** and **B** presented in Scheme 8 were compared by using *ab-initio* quantum-chemical calculations. The differences in the total energies of the optimized molecules show a clear preference for pathway **A** with only 119.9 kJ mol^{−1}, compared with 692.2 kJ mol^{−1} for pathway **B** (Fig. 6). The donor-stabilized silylene species and MeSiCl₃ in **A** are far more stable than the donor-stabilized silicenium ion and the free silylene in **B**.

It is well known that silylenes, similarly to carbenes, undergo insertion reactions in E–X bonds (E=B, P, C, Si; X=H, Cl, OR).¹¹⁸ First, disilane **2** acts as a reservoir on the catalyst surface for the insertion of silylenes into Si–Cl bonds, which accounts for the formation of the trisilane **3**. Moreover we tried to get further information about the quantum-chemical properties of the higher oligosilanes to explain the favored formation of branched silicon backbones. The search for the optimum structure of **3** is a complex problem. In a first stage, a

Table 3 Calculated values of total energy as well as HOMO and LUMO energies for selected molecules

Molecule	Total energy (Hartree)	HOMO (eV)	LUMO (eV)
Cl ₂ MeSi—SiMeCl ₂ (2)	− 2 483.658 149 8	− 11.00	3.01
O=PH ₃	− 415.266 041 9	− 11.70	5.40
H ₃ P=→Cl ₂ MeSi—SiMeCl ₂ (19)	− 2 898.957 430 0	− 10.13	2.88
H ₃ P=O→SiMeCl	− 1 199.625 658 2	− 7.45	3.33
[H ₃ P=O→SiMeCl ₂] ⁺	− 1 656.948 333 0	− 16.35	− 1.77
Cl ₃ SiMe (1)	− 1 699.286 161 4	− 12.60	4.47
Cl [−]	− 457.444 119 5	− 3.12	25.93
Cl ₂ MeSi—SiMeCl—SiMeCl ₂ (3)	− 3 268.029 646 4	− 10.54	2.25
MeSiCl	− 784.301 322 7	− 9.17	0.693

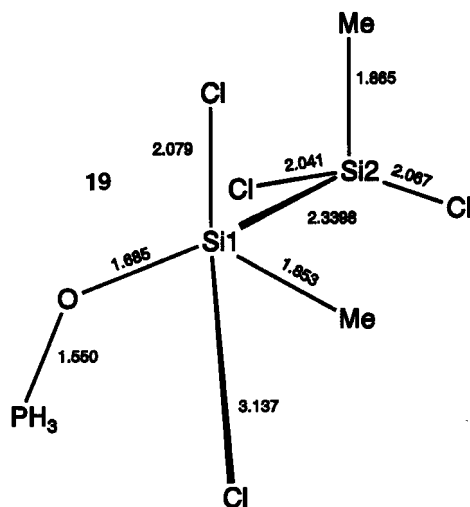


Figure 5 Bond distances (Å) in **19**.

conformer search based on the Sybyl force field was performed. The minimum conformer obtained was submitted to an *ab-initio* geometry optimization with the 3-21G(*) basis set and the resulting minimum structure was verified by calculating the Hessian matrix. The analysis of the frontier orbital energies of **2** and **3** shows a lowering of the LUMO energy for the trisilane. This should enable the reactive silylene intermediate to react preferentially with the trisilane

as depicted in Fig. 7. It is possible to show by molecular orbital analysis that the LUMO of **3** is mainly localized on the central silicon atom (32%) and that there is only a minor part of it on the terminal silicon atoms (6% and 19%). The reactive silylene species should therefore attack mainly at the central silicon atom; this is in excellent agreement with the experimental results. The central Si-Cl bond of **3** seems to be the most effective trap for the silylene, causing the extraordinary high regioselectivity for the formation of the branched tetrasilane **4** [Eqn 26].

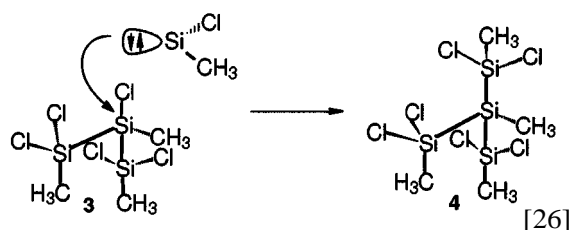
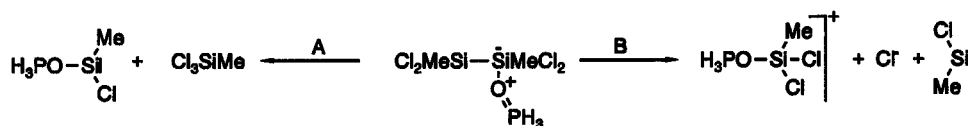


Figure 6 Energy profiles of reaction pathways A and B.

Former interpretations have elucidated the formation of **3** via a concerted reaction in which a four-center transition state is created stabilized by Lewis bases¹¹⁰ (Scheme 9a). However, since the formation of branched silicon backbones (**4**) is strongly favored, a four-center transition state should form with secondary silicon atoms; this is already sterically very demanding (Scheme 9b),



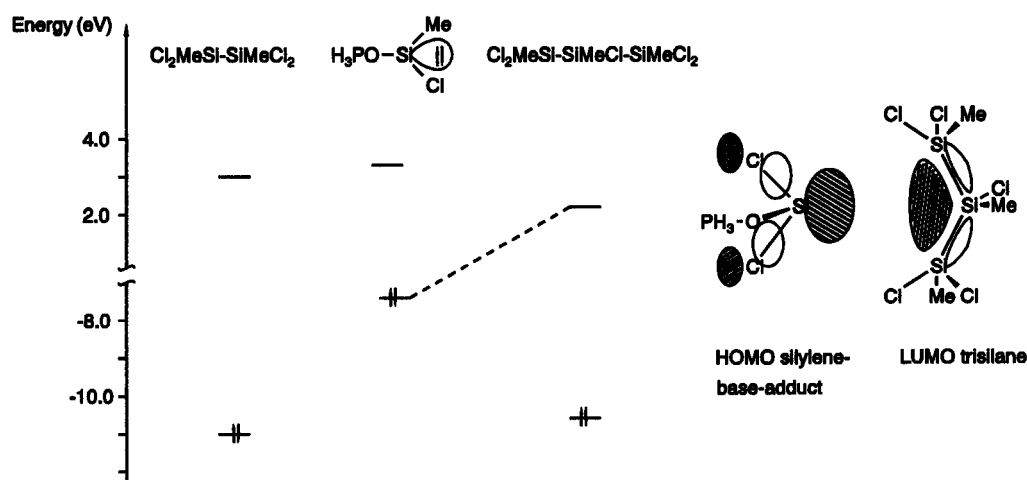
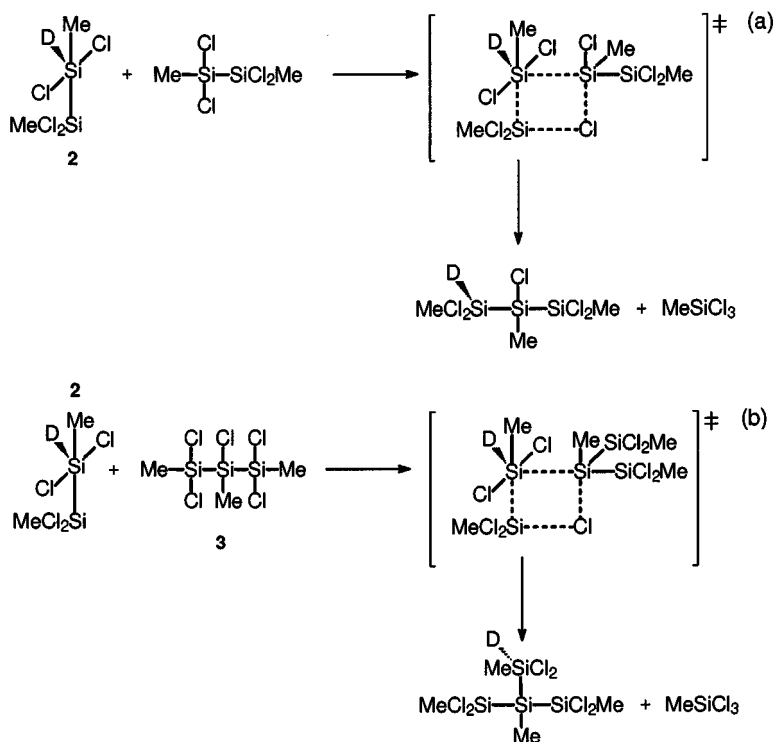


Figure 7 Frontier orbital energies of **2**, **3** and the silylene intermediate, and shapes of the LUMO of **3** and of the HOMO of the silylene intermediate.

so the proposed mechanism seems to be quite improbable.

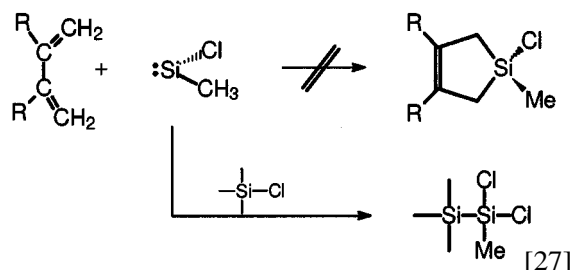
Silylene trapping experiments in condensed phase with diolefins such as dimethylbutadiene, which are expected to form the Diels–Alder product 1-chloro-1-methyl-3,4-dimethylsilacy-

clopent-3-enes, have been unsuccessful so far. Such reactions have been reported for thermally generated silylenes (500–550 °C) in a stream of butadiene.¹¹⁹ In the present case, however, the cyclization reaction seems to be prevented due to competing insertion reactions of silylenes into



Scheme 9. Proposed four-center transition states for the disproportionation (a) of **2** and (b) of **2** and **3**.

Si–Cl bonds (Eqn [27]).



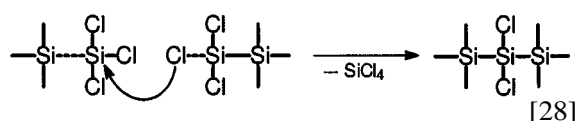
Closer observation of the proposed mechanisms for dehydropolymerization of disilanes and catalytic disproportionation of halodisilanes suggests that silylenes obtained by Si–Si bond cleavage are obviously key intermediates for the formation of various polysilane skeletons. This conclusion is supported by the analogue spectrum of reaction products consisting of branched oligomers and polymers. The silylenes, despite bearing different substituents (Me, Cl, H, OMe, etc.), undergo the same kind of reaction: insertion into Si–X (X=Cl, H, etc.) bonds. At first sight the generation of the silylene intermediates seems to be different (metal complex, Lewis base).

However, the formation of the respective silylenes can be generalized if a first electron-transfer step is assumed (Scheme 10). This assumption is supported by very recent investigations on electrochemical reactions of organosilanes¹²⁰ and on dehydropolymerization of organodisilanes using reducing catalyst systems such as $\text{Cp}_2\text{MCl}_2/\text{Red-Al}$ {M=Ti, Hf; $\text{Red-Al}=[(\text{MeOCH}_2\text{CH}_2\text{O})_2\text{AlH}_2]\text{Na}$ }.¹²¹ As shown in this paper, the electron source may be different: metal, metal complexes, a cathode or Lewis bases. The coordinative stabilization of the silylenes formed is provided by the presence of the metal complex or the Lewis base. It could act as an additional driving force to prevent

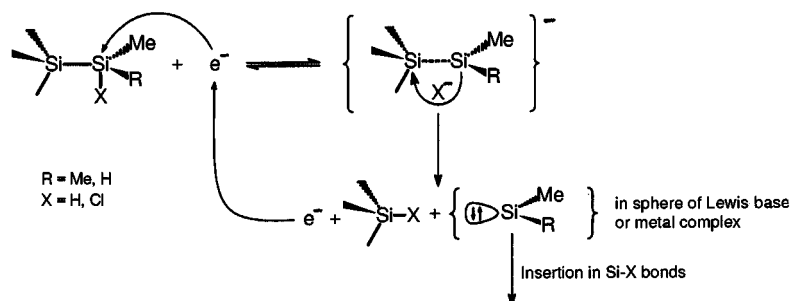
reverse reactions and also to influence orbital symmetries.

2.5.1 The formation of poly(chloromethylsilane)s-branching and crosslinking reactions

The number of Cl atoms bonded to silicon – $\text{SiCl}_{3-x}\text{Me}_x$ ($x=0, 1, 2$) in chloromethyldisilanes dictate the nature of the structural units present in the oligo- or polysilanes (Table 4). Thus quaternary, tertiary or secondary silicon backbone atoms can be obtained by variation of the functionality of the disilanes. This is also valid for polysilanes derived from the oligomers through branching and crosslinking reactions. First direct indications of such second polymerization mechanisms were found in the disproportionation of $\text{MeCl}_2\text{Si}-\text{SiCl}_3$ into neo- $\text{Si}_5\text{Cl}_{11}\text{Me}$ and MeSiCl_3 Eqn [16].⁹⁸ In addition, a polymeric residue with an average $\text{SiCl}_{1.03}\text{Me}_{0.7}$ composition and the evolution of SiCl_4 were observed. The latter is obviously generated in the reaction of oligosilanes with each other, in which the Cl exchange proceeds intermolecularly causing an Si–Si bond cleavage (Eqn [28]).

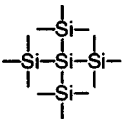
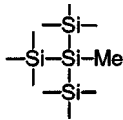
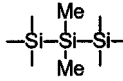


We obtained similar indications during the heterogeneous disproportionation of **2**. As already mentioned, the trisilane **3** and isotetrasilane **4**, obtained free from catalyst, undergo thermally induced branching reactions giving higher oligomers **5**, **6** and **7** at reaction temperatures of 160–175 °C.^{97,114} The reaction course is not yet completely understood, nor is the role of the monosilane MeSiCl_3 which it is suggested may have a catalytic influence on such a branching or crosslinking process. For exam-

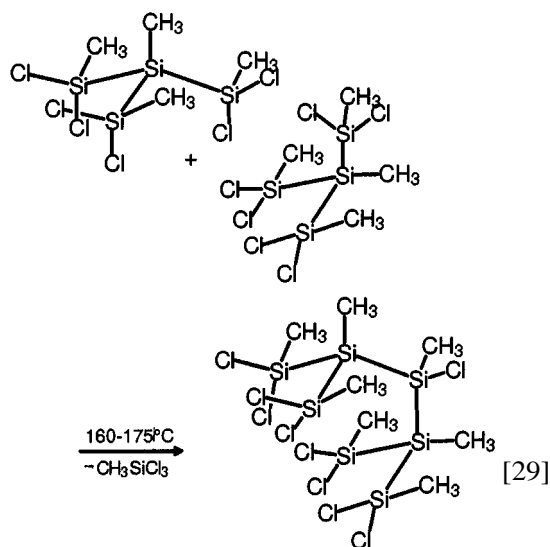


Scheme 10. Generation of silylenes by electron-transfer steps.

Table 4 Characteristic structural Si units of polysilane backbones derived from halosilanes

Silyl group of halosilane	Backbone unit	Si atom
– SiCl ₃		Quaternary
– SiCl ₂ Me		Tertiary
– SiClMe ₂		Secondary

ple, the formation of **7** is apparently due to the branching reaction of isotetrasilanes **4** in connection with loss of MeSiCl₃ (Eqn [29]).



If the temperature is increased slightly to 180–185 °C, the branching is accompanied by crosslinking in which inter- and intra-molecular cyclization processes occur, causing a drastic increase of the reaction mixture viscosity. The chemical species present in the reaction mixture cannot be identified any more by common solution-NMR/spectroscopic methods during that period of reaction, because of the enlarged number of product molecules and conformational isomers as well the transition to a

polymeric network. After 2 h of reaction and subsequent cooling at room temperature, a solid polymer (PCMS 180) with an average SiMeCl_{0.62} composition is obtained. The yellowish transparent polymer is meltable and soluble in organic solvents such as toluene, THF, CCl₄ or CHCl₃.

A similar access route to poly(chloromethylsilane)s was first demonstrated by Baney *et al.* via homogeneous catalytic disproportionation of chloromethyldisilanes (MeCl₂Si)₂ and Me₂ClSiMe using ¹Bu₄PCl as catalyst.¹³ The assumed five- and six-membered silicon structure of the resulting polymer heat-treated up to 250 °C was derived from an empirical formula of (MeSi)_{5.7}(Me₂Si)_{1.0}Cl_{1.9} with an average number of Si–Si bonds of 2.65/Si, indicating a high level of crosslinking. Using ebulliometry for molecular-weight determination an average value of 1000–1300 was obtained. Spectroscopic identification of the various polymer silicon and carbon backbone sites was unsuccessful due to broad and ill-defined NMR resonance peaks.

2.5.2 NMR investigation of the crosslinking process of poly(chloromethylsilane)s

The structure of the solid polymer obtained after 2 h at 180 °C (PCMS 180) was investigated by ²⁹Si and ¹³C MAS–NMR using cross-polarization (CP) but also inversion recovery cross-polarization (IRCP). These experiments have been described in detail elsewhere^{122,123} and will be only briefly summarized in this paper. Series of spectra with variable contact times (CP) and inversion time (IRCP) were recorded and simulated to extract very accurately the various resonance peaks. Then the dynamics of polarization inversion in the IRCP experiments was analyzed according to previously developed models.^{124,125} One characteristic time that can be extracted through a fitting procedure is related to dipolar couplings between the observed nucleus (²⁹Si or ¹³C) and protons, and is thus sensitive to the proton environment as well as to the mobility of the observed groups. Then the dynamics of cross-polarization in the CP experiments was analyzed in a similar way,¹²⁶ leading to a quantification of the various ²⁹Si or ¹³C sites.

The ²⁹Si and ¹³C CP MAS–NMR spectra of PCMS 180 are presented in Figs 8(a) and 8(b). The resonance peaks extracted from the simulations are summarized in Table 5, together with their relative intensities. The assignments of the silane units have been obtained by comparison with the solution NMR performed on the oligosi-

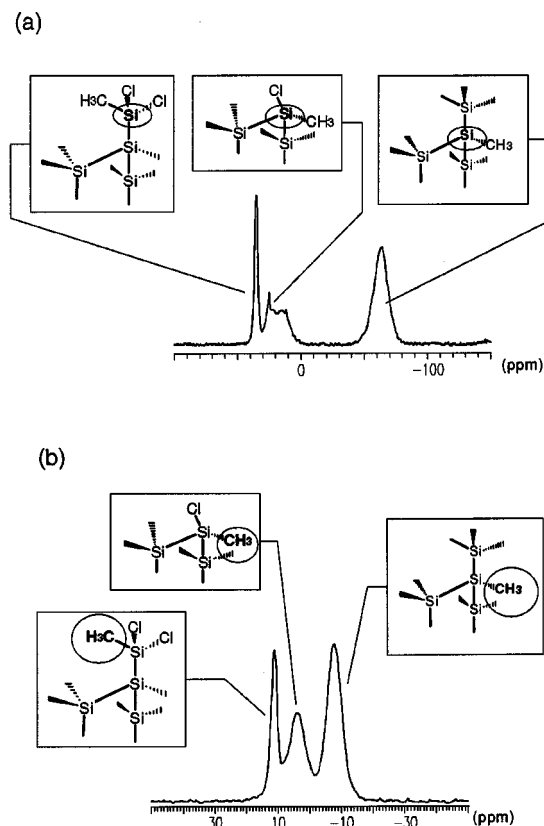


Figure 8 (a) ^{29}Si CP MAS-NMR spectrum of PCMS 180 recorded with a contact time of 5 ms; (b) ^{13}C CP MAS-NMR spectrum of PCMS 180 recorded with a contact time of 1 ms.

lanes 2–7,⁹⁷ and clearly show the presence of tertiary $\text{MeSi}(\text{Si})_3$, linear $\text{MeClSi}<$ and terminal $\text{MeCl}_2\text{Si}-$ units. A small ^{29}Si resonance peak has been tentatively assigned to carbosilane sites $-\text{CH}_2\text{Si}(\text{Si})_3$; this assignment has been discussed previously.¹²³ The average composition $\text{SiMeCl}_{0.73}$ is in quite good agreement with the result of mass balance analysis ($\text{SiMeCl}_{0.62}$). The quantification of the different structural units

Table 5 Comparison between ^{29}Si and ^{13}C NMR data on PCMS 180 and proposed assignments

^{13}C NMR		^{29}Si NMR		Assignment
δ (ppm)	(%)	δ (ppm)	(%)	
-7.6	46	-64.0	46	$(\text{Me})\text{Si}(\text{Si})_3$
		-51.2	3	$(-\text{CH}_2)\text{Si}(\text{Si})_3$
4.1	35	14.1	18	$\text{MeClSi}<$
		24.2	10	
11.4	19	35.3	23	$\text{MeCl}_2\text{Si}-$

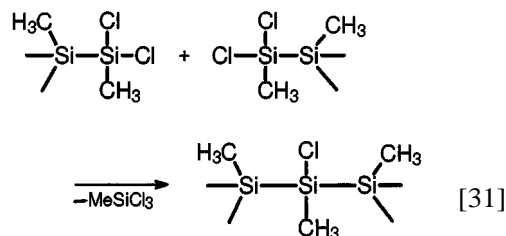
allows the calculation of the degree of cross-linking of the polysilane network (C.D.) according to:

C.D. =

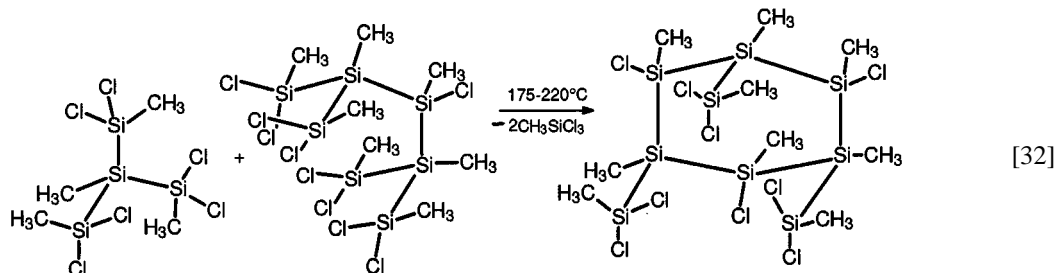
$$\frac{3[\text{MeSi}(\text{Si})_3] + 2[\text{MeClSi}<] + [\text{MeCl}_2\text{Si}-]}{100} \quad [30]$$

where the concentrations are expressed as percentages. In the case of PCMS 180, a C.D. value of 2.2 indicates an extended state of cyclization. Unlike dehalocoupling, the Si-Cl groups are predominantly retained during the disproportionation. They are the centers for thermally induced crosslinking, that can be explained by the following condensation reactions.

(a) Condensation of terminal silyl groups $-\text{SiCl}_2\text{Me}$:

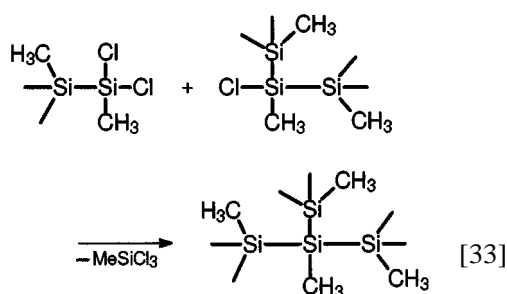


Silylene $>\text{SiClMe}$ units are formed in the course of the reaction depicted in Eqn [31]. Since the silyl groups are mainly bonded to tertiary silicon atoms, the

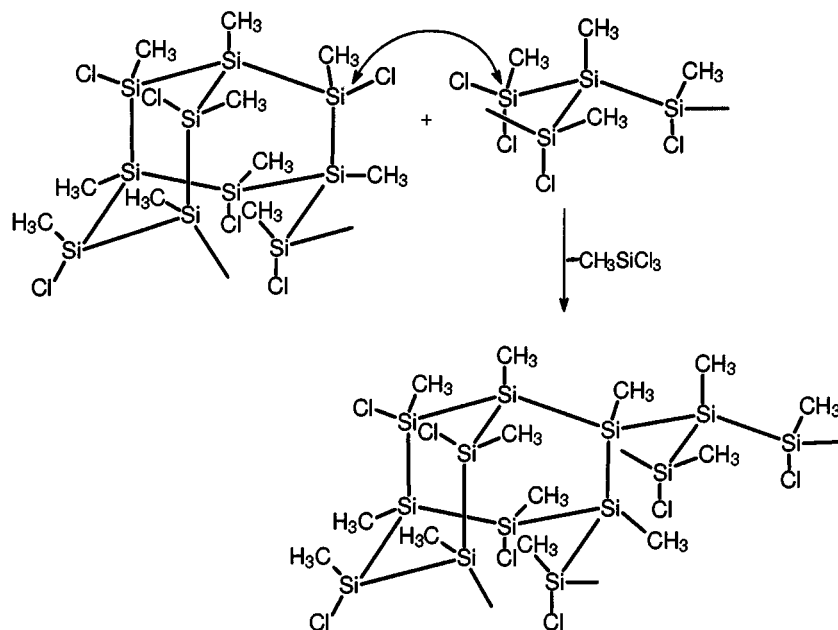


silylene groups obtained have two tertiary-silicon neighbours. This kind of crosslinking is strongly suggested to be responsible for general cyclization reactions such as that illustrated in Eqn [32].

- (b) Condensation of silyl $-\text{SiCl}_2\text{Me}$ and silylene groups $>\text{SiClMe}$ generating branched (tertiary) silicon backbone atoms $\text{Me}-\text{Si}(\text{Si})_3$:



According to Eqn [33], the chlorine donor is the silylene site. Such a reaction can be tentatively understood as a branching or linking reaction between polysilane ring systems leading finally to a 3D polysilyne-type polymer architecture, probably constituted by predominantly fused six-membered rings. A part of such architecture is depicted schematically in Eqn [34].



A further increase of the reaction temperature to 450°C causes considerable changes in the polymeric silicon backbone which can be clearly monitored by ^{29}Si and ^{13}C MAS-NMR (Figs 9 and 10). All the resonance peaks broaden out due to a large distribution of ^{29}Si as well as ^{13}C sites caused by extensive crosslinking reactions. Moreover, new ^{29}Si resonance peaks are clearly present between 0 and -50 ppm, in a chemical shift range corresponding to carbosilane units. For each temperature a detailed analysis of the ^{29}Si CP and IRCP experiments, as previously summarized, was done:¹²³ identification and quantification of the various overlapping resonance peaks were achieved for each reaction temperature. The analysis of the dynamics of polarization inversion shows a clear difference in behavior between peaks due to silane units and the new peaks, and thus allows tentative assignment of these peaks to various carbosilane units, as reported in Table 6. A new peak around $-105/-110$ ppm is also present in samples treated at $T > 300^\circ\text{C}$, due to quaternary silane units $\text{Si}(\text{Si})_4$. Their presence seems to be closely related to the formation of carbon-rich carbosilane units in samples with a relatively low C/Si molar ratio.

Formation of carbosilane units is obviously related to the formation of CH_2 groups that should be identified in the ^{13}C NMR spectra (Fig.

10), but the strong overlapping of the ^{13}C resonance peaks makes a direct identification of the peaks impossible. IRCP experiments are of great interest to solve such problems: as already mentioned, the dynamics of polarization inversion strongly depends on ^{13}C – ^1H dipolar

coupling and thus should allow a clear distinction between the various $^{13}\text{CH}_x$ sites depending on the value of x . After a detailed analysis of the IRCP spectra,^{122,123} unambiguous identification of a broad resonance peak around 9 ppm due to CH_2 groups was done for samples treated at

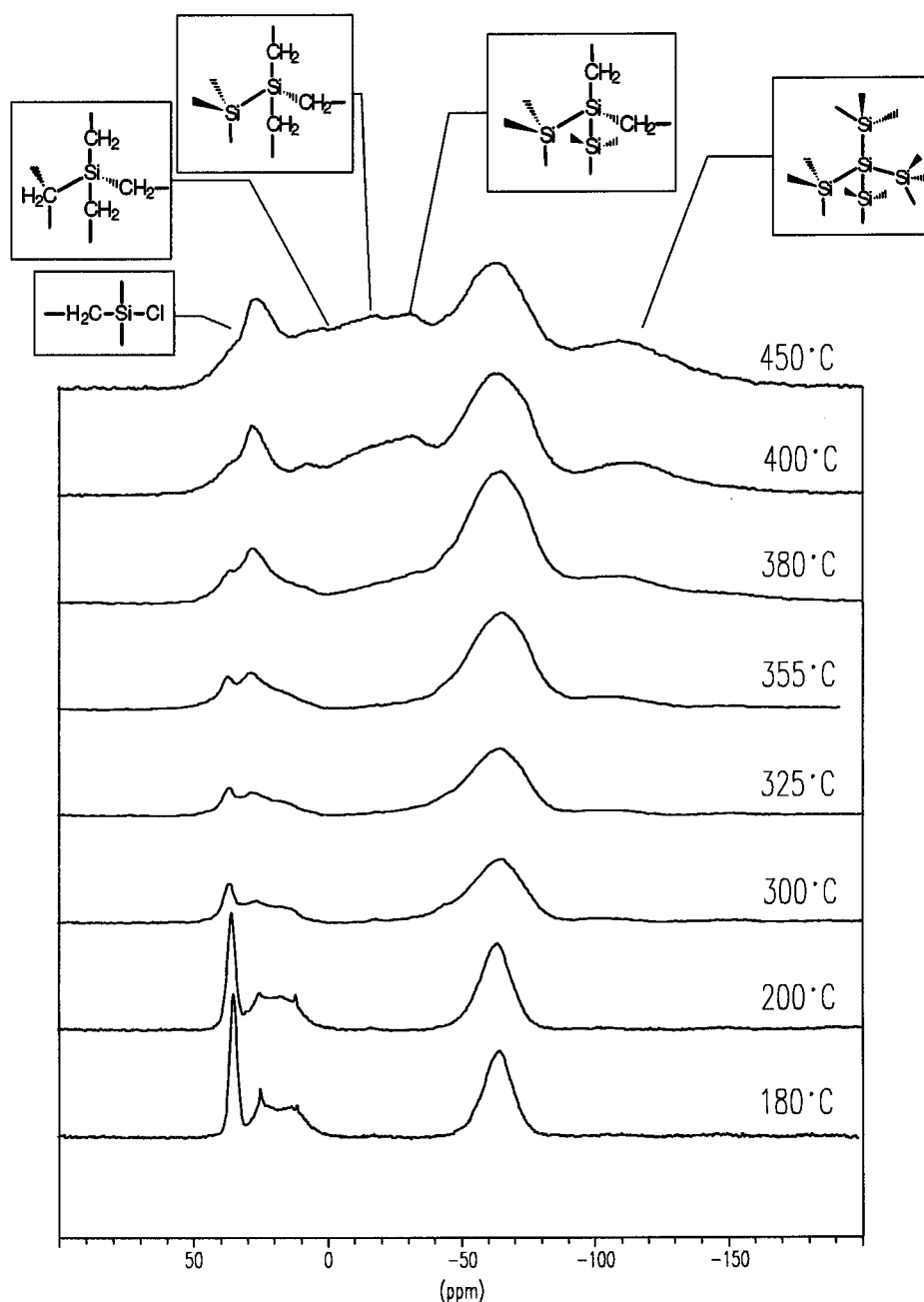


Figure 9 ^{29}Si CP MAS-NMR spectra of the poly(chloromethylsilane)s treated at various temperatures (contact time: 5 ms).

$T \geq 380^\circ\text{C}$. Assignments of the various ^{13}C resonance peaks are summarized in Table 7.

From the quantitative analysis of the ^{29}Si NMR spectra it is possible to estimate the number of Si-Cl, Si-Si and Si-C bonds per Si atom for each reaction temperature (Fig. 11). The

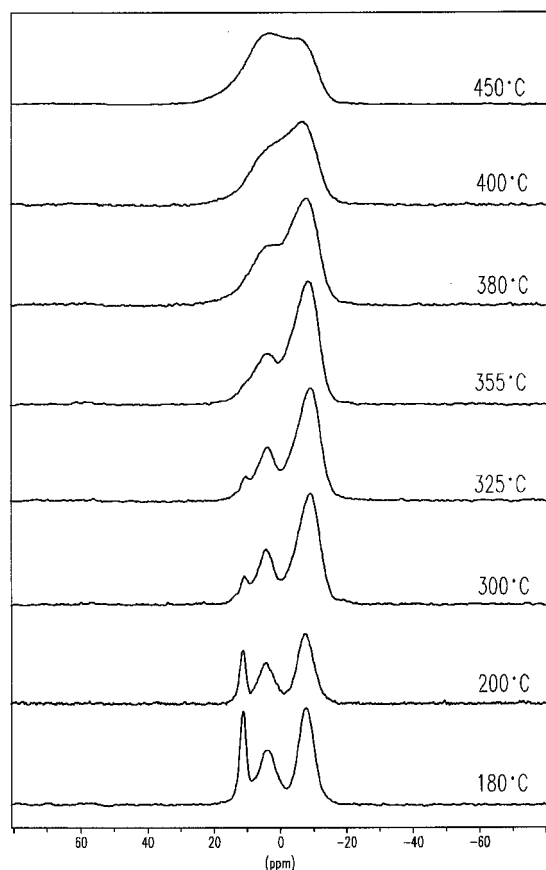
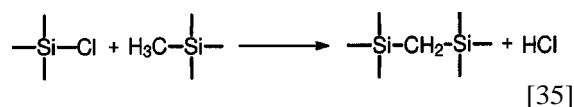
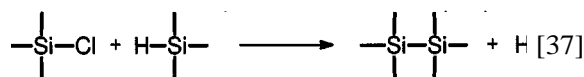
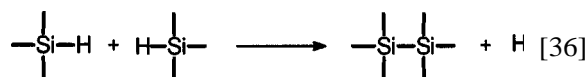


Figure 10 ^{13}C CP MAS-NMR spectra of the poly(chloromethylsilane)s treated at various temperatures (contact time: 3 ms).

two main temperature ranges can be distinguished: from 180°C to 350°C the number of Si-bonds remains constant while the decrease in Si-Cl bonds occurs simultaneously with an increase in Si-Si bonds. This corresponds to crosslinking reactions which transform terminal and linear units into tertiary units, leading to a highly condensed polysilane network. Then, from 350°C to 450°C , the polysilane-to-poly(carbosilane) transformation clearly occurs, indicated by a decrease in the number of Si-Si bonds and an increase in Si-C bonds. The carbosilane units can be formed either from Si-Me and Si-Cl groups (Eqn [35]) with HCl evolution or through the Kumada rearrangement Eqn [7].



In this temperature range the Cl content does not vary too much and the carbosilane units seem to originate from tertiary units, suggesting that the Kumada rearrangement occurs. However, no Si sites with Si-H bonds were identified through the IRCP experiments, which should be very sensitive to this kind of site.¹²³ Possibly Si-H entities that are formed primarily may react subsequently leading to formation of H_2 (Eqn [36]) or HCl (Eqn [37]).



Indeed, in this temperature range not only HCl but also hydrogen are detected in thermogravi-

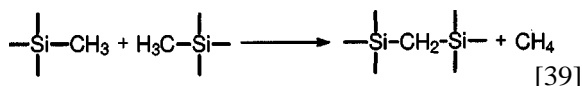
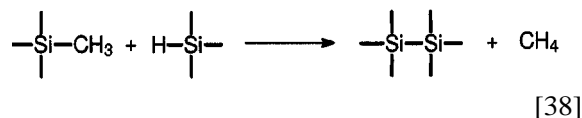
Table 6 Proposed assignments for the ^{29}Si resonance peaks

Assignment	δ range (ppm)
Tertiary units $\text{MeSi}(\text{Si})_3$	-60/-70
Linear units MeClSi	15/40
Terminal units MeCl_2Si	35/40
Quaternary units $\text{Si}(\text{Si})_4$	-105/-110
Carbosilane units $(\text{—CH}_2)\text{Si}(\text{Si})_3$	-45/-50
Carbosilane units $(\text{—CH}_2)_x\text{Me}_{2-x}\text{Si}$ ($x=1, 2$)	-30/-35
Carbosilane units $(\text{—CH}_2)_x\text{Me}_{3-x}\text{Si}$ ($x=2, 3$)	-10/-15
Carbosilane units $(\text{—CH}_2)_x\text{Me}_{4-x}\text{Si}$ ($x=3, 4$)	0/10
Carbosilane units $(\text{—CH}_2)\text{MeClSi}$	25/30

Table 7 Proposed assignments for the various ^{13}C resonance peaks

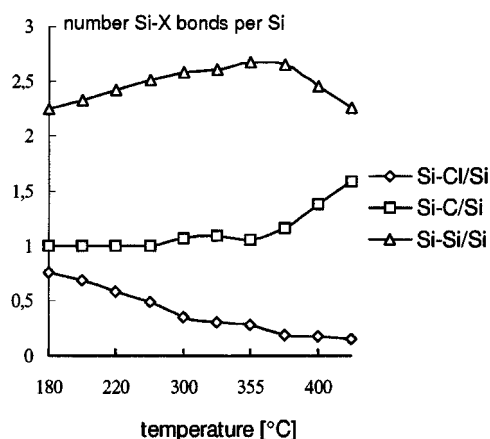
Assignment	δ (ppm)
$\text{MeSi}(\text{Si})_3$	-7/-9
$\text{MeClSi} <$	3/4
MeCl_2Si	11
$\text{MeSi}(\text{Si})_3$	-4/-6
MeSiCH_2-	4/6
$-\text{SiCH}_2-$	9

metric analysis coupled with mass spectrometry.¹²³ Methane is also formed and can result according to Eqn [38] or [39].



2.6 Disproportionation in presence of olefins

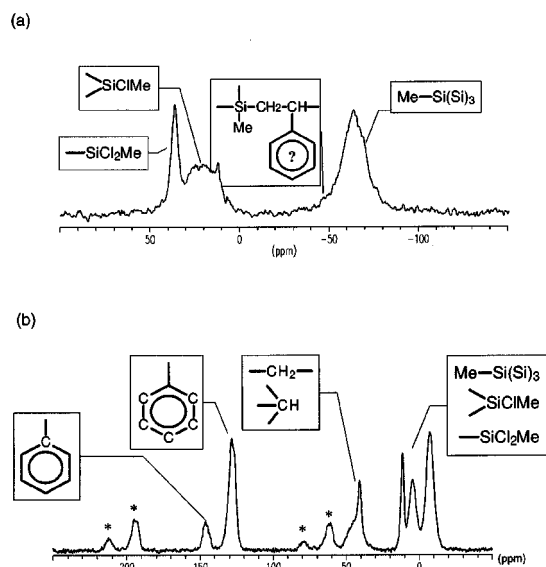
The synthesis of hydrocarbon-co-polymeric silanes or carbosilanes can be achieved by combined polymerization of organic monomers and metal-induced dehalocoupling of halo-organosilanes. Suitable organic monomers are

**Figure 11** Variation with reaction temperature of the number of Si—Cl, Si—C and Si—Si bonds per Si atom, extracted from the ^{29}Si NMR results.**Table 8** Average polymer compositions^a of various poly-(chloromethylsilane-co-styrene)s

Polymer	C_8H_8 ^b (mol%)	Si (wt%)	C (wt%)	H (wt%)	Cl (wt%)
CoP 5	5.16	43.8	26.8	5.1	21.4
CoP 10	9.90	37.4	31.7	5.7	24.7
CoP 18	17.67	31.8	42.4	5.3	17.8
CoP 25	24.64	27.8	53.3	6.1	12.3
CoP 30	30.40	22.4	55.1	5.9	17.2

^a The accuracy of the mass balance analysis decreases with increasing Si content because of SiC formation during combustion analysis, which could not be completely avoided yet.

^b Ratio of styrene to **2** in the parent mixture.

**Figure 12** (a) ^{29}Si CP MAS-NMR spectrum of poly-(chloromethylsilane-co-styrene) (CoP 18) (contact time, 10, ms) and (b) ^{13}C CP mas-NMR spectrum of the same polymer (contact time, 3 ms; * spinning side bands).**Table 9** Ostwald coefficients of poly(chloromethylsilane-co-styrene)s

Polymer	m
CoP 10	0.5
CoP 18	0.55
CoP 25	0.7

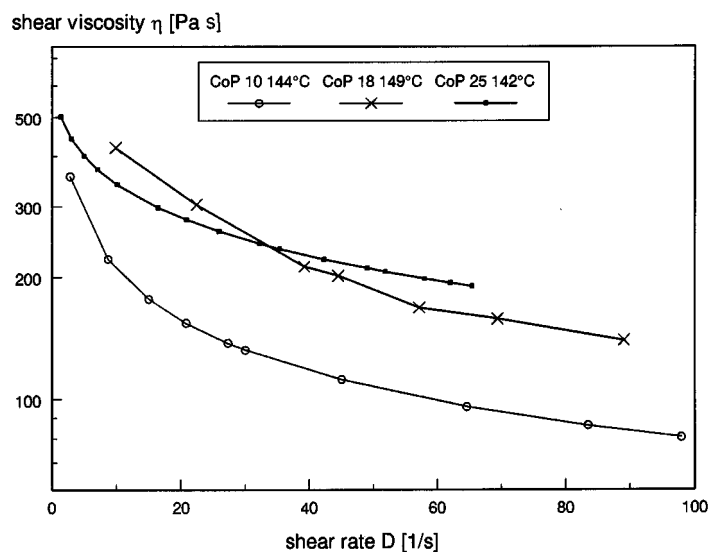
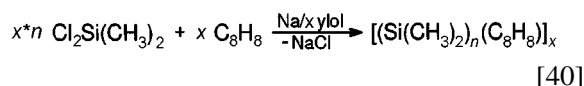


Figure 13 Dependence of shear viscosity on shear rate of various poly(chloromethylsilane-co-styrene)s.

styrene, α -methylstyrene or conjugated olefins such as butadiene or isoprene.^{127–129} Sartori and co-workers investigated the incorporation of styrene in polysilane backbones by variation of the styrene content:¹³⁰



In the case of a low styrene concentration in the starting reaction mixture, the incorporated phenylethylene groups are randomly distributed in the polymer skeleton.

It is well known that silylenes can be added to alkenes or alkynes.^{118,130} As an example the reaction between dimethylsilylene and ethylene carried out in condensed phase leads to vinyl dimethylsilane and also to polymeric products. [Eqn [41]]. Silacyclopropanes (siliranes) are considered as potential reactive intermediates.

In the light of these investigations it is interesting to know whether the silylenes generated from $\text{MeCl}_2\text{Si-SiCl}_2\text{Me}$ (**2**) undergo an addition reaction to styrene on the catalyst surface, or whether the silylene insertion into Si-Cl bonds is absolutely favored. In order to introduce phenylethylene units into the poly(chloromethylsilane) network, the styrene content was varied in the starting mixture with **2** (Eqn [42]). The only gaseous product detected at reaction temperatures between 150 and 220 °C was the monosilane MeSiCl_3 . After 2 h of reaction at 220 °C and subsequent cooling at room temperature, solid styrene-containing poly(chloromethylsilane)s were obtained. The yellowish homogeneous polymers are meltable and soluble in common organic solvents such as toluene, chloroform or THF. The mass balance analysis results are summarized in Table 8.

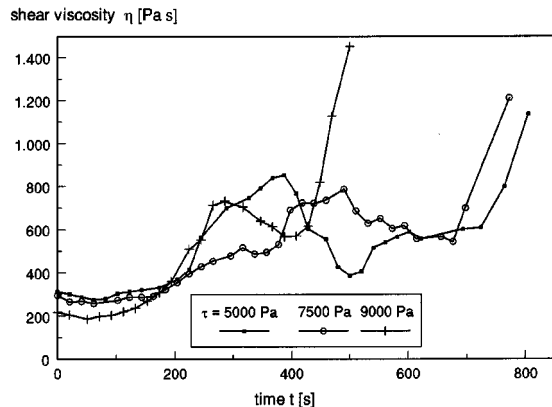
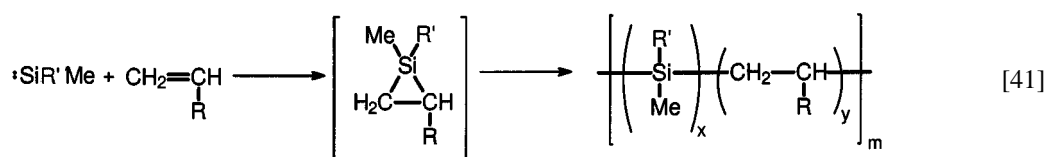


Figure 14 Shear viscosity versus time for poly(chloromethylsilane-co-styrene) (CoP 25).

Table 10 Average loss factors of poly(chloromethylsilane-co-styrene)s

Polymer	Δ_1 at $\omega=31.4$ Hz	Δ_2 at $\omega=62.8$ Hz	Δ_1/Δ_2
CoP 10	1.6	1.0	1.6
CoP 18	2.0	1.1	1.8
CoP 25	2.5	1.25	2.0



Structural investigations by ^{29}Si and ^{13}C MAS-NMR have been performed on CoP 18 to search for possible bonding between the silane and the styrene units. The ^{29}Si CP MAS-NMR spectrum (Fig. 12) is very similar to that obtained for PCMS 180 (Fig. 8a). No resonance peaks due to Si units bonded to styrene groups were clearly identified, so if such bonds do exist they should be present in small amounts, i.e. only <5%.

The ^{13}C CP MAS-NMR spectra were recorded with variable contact times in order to quantify the silane and styrene moieties (Fig. 12b). All the peaks can be assigned either to polysilane units or to polystyrene units. The calculated ratio between styrene monomers (18.5 mol%) and silane units is in very good agreement with that of the starting mixture (17.7 mol%), indicating the complete incorporation of the styrene units in the final product. Detailed IRCP investigations with variable inversion times to search for possible CH_2 or CH groups belongs to styrene entities bonded to Si units were performed without success. The corresponding resonance peaks should overlap the resonance peaks due to the methyl groups bonded to silane units, but should be identified by IRCP techniques if a reasonable amount is present (<5%).

Both ^{29}Si and ^{13}C NMR investigations, despite a detailed analysis of CP and IRCP experiments, have so far been unsuccessful in identifying bonds between polysilane and polystyrene moieties. Consequently it is currently difficult to decide whether a copolymer constituted by long blocks is formed. Size-exclusion chromatography investigations that are currently in progress may give a better insight into the polymer

structure and the polymer formation mechanism. However, these investigations are difficult to perform because of the high polymer reactivity and especially because of the lack of comparable standards. This is also a reason why no weight- and number-average molecular weight distributions can be reported so far.

The NMR results confirm the assumption that silylenes do not react in reasonable amounts with olefins under the specific disproportionation conditions on the catalyst surface at temperatures between 125 and 150 °C. Nevertheless the reactive Cl-containing polymers obtained show very interesting properties as precursors for SiC materials, especially for SiC fibers.

2.6.1 Rheology and spinning

Continuous polymer fibers were drawn from molten poly(chloromethylsilane-co-styrene)s under an argon atmosphere. A precise temperature setting is important for the success of the spinning procedure, but very difficult to realize. The polymer melting temperature ranges are very sensitive to polymers synthesis conditions (thermally induced crosslinking) and vary in a range between 115 and 150 °C. In general the spinning behavior improves with increasing styrene content. Thus CoP 25 with 24.6 mol% styrene content shows excellent spinnability to continuous fibers.

The polymer spinnability can be defined as the maximum attainable filament length; this is limited by two processes:¹³²

- (1) Cohesion break depends on the viscosity, the elastic modulus, the cohesion energy of the substance and the velocity of fiber stretching.

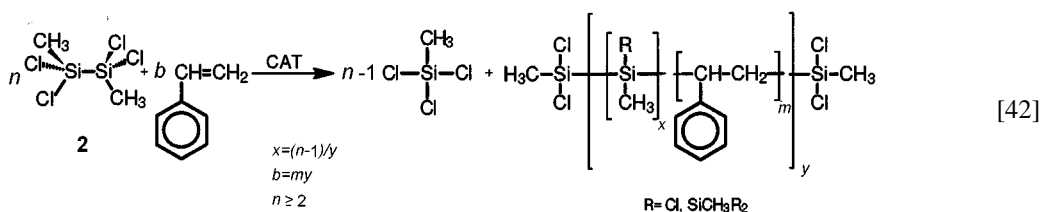


Table 11 Properties of SiC fibers derived from poly-(chloromethylsilane-co-styrene) (CoP 18)

Diameter	15–30 μm
Tensile strength	600–2100 MPa
Thermal resistance (in air)	1500 $^{\circ}\text{C}$
Crystallite size	
X-ray amorphous	1200 $^{\circ}\text{C}$
2 nm	1400 $^{\circ}\text{C}$
10 nm	1600 $^{\circ}\text{C}$
Electrical conductivity	Semiconductive
Density	2.5 g cm^{-3}
C/Si ratio	1.05:1
Oxygen	<1wt%
Nitrogen	<5wt%
Chlorine	<1wt%
Free carbon	<3wt%

- (2) Capillary break is caused by elastic surface waves and depends on the viscosity, the deduction rate and the surface tension of the material.

Rheological parameters of reactive organosilicon polymers have not been reported so far. Therefore it is essential to investigate the dependence of shear viscosity on shear stress or shear rate and temperature, as well as to find out the magnitudes of the viscous (loss modulus) and elastic (storage modulus) ratios and their depend-

ence on strain and temperature. The results of these rheological investigations should give a first tentative insight into the physical properties of the polymers.

Polymer shear viscosities η commonly depend on the applied shear stress and can be described by flow curves measured in rotary experiments by varying either shear stress or shear rate. Non-Newtonian fluids are described by the Ostwald model:

$$\tau = \eta D^m \quad [43]$$

where τ is the shear stress (Pa), D is the shear rate (s^{-1}) and the Ostwald coefficient m is an indication of the extent of stress dependence. It is between 0 and 1 for the poly(chloromethylsilane-co-styrene)s and increases with the styrene content from CoP 10 to CoP 25 (Table 9). Ostwald coefficients smaller than 1 means a decrease of shear viscosity with the shear rate, called shear thinning or non-Newtonian behavior, as depicted in Fig. 13. The temperatures at which these experiments were performed were chosen according to the melting temperature range of the various polymers and the spinning experiment conditions.

The shear viscosity–time experiment (Fig. 14) performed under an inert atmosphere demonstrates the self-crosslinking behavior of the CoP

Table 12 Experimental data for the disproportionation of $\text{MeCl}_2\text{Si}-\text{SiCl}_2\text{Me}$ (**2**)

Polysilane	Parent 2 (g) [mol]	T_R^a ($^{\circ}\text{C}$)	t_R^b (h)	Polymer yield (wt%)	F_r^c ($^{\circ}\text{C}$)
PCMS 180	78 [0.34]	180	2	22.8	110–125
PCMS 220	61.5 [0.27]	220	2	23.7	165–180

^a Maximum reaction temperature.

^b Holding time at T_R .

^c Melting range.

Table 13 Experimental data for the synthesis of poly(chloromethylsilane-co-styrene)s from starting mixtures of $\text{MeCl}_2\text{Si}-\text{SiCl}_2\text{Me}$ (**2**) and styrene

Polymer	2 (g) [mol]	C_8H_8 (g) [mol]	Polymer yield (wt%)	F_r ($^{\circ}\text{C}$)
CoP 5	88.1 [0.39]	2.2 [0.02]	20.5	125–135
CoP 10	64.7 [0.28]	3.2 [0.03]	26.7	130–150
CoP 18	121.3 [0.53]	11.9 [0.11]	30.8	120–130
CoP 25	82.2 [0.36]	12.3 [0.12]	29.5	125–150
CoP 30	52.3 [0.23]	10.4 [0.1]	31.9	115–150

caused by shear stress. When the polymer melt is subjected to a constant shear stress τ , the shear viscosity remains constant during only a short period of time and then increases up to hardening. The higher the applied shear stress, the quicker the hardening.

As already mentioned, the elastic ratio of the polymer melt affects the polymer spinnability. Too high an elasticity causes corkscrew-like fibers; low elasticity leads to filament breakage.

The viscoelastic behavior of the polymers can be examined by oscillation experiments. The polymers are subjected to a sinusoidal strain according to Eqn [44]:

$$\gamma(t) = \gamma_0 \sin \omega t \quad [44]$$

where γ denotes the strain, γ_0 the strain amplitude and ω the radial frequency. The measured stress curve can be described by Eqn [43]. Viscoelastic fluids re-deform incompletely and with a time delay, caused by the viscous ratio. This phenomenon corresponds in the stress equation to the phase-shift angle δ_s ,

$$\tau(t) = \tau_0 \sin(\omega t + \delta_s) \quad [45]$$

where τ_0 is the stress amplitude.

The determined viscous and elastic ratios can be expressed in terms of the loss (G'') and storage (G') moduli:

$$G'' = (\sin \delta_s) \tau_0 / \gamma_0 \quad [46]$$

$$G' = (\cos \delta_s) \tau_0 / \gamma_0 \quad [47]$$

The relation between viscous and elastic ratios is defined as the loss factor Δ :

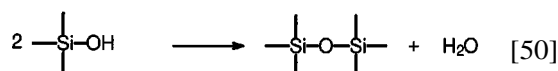
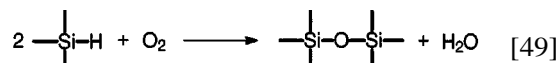
$$\Delta = \tan \delta_s = G'' / G' \quad [48]$$

Before any investigations are carried out on the elastic and viscous ratios, the linear viscoelastic range for the poly(chloromethylsilane-co-styrene) melts has to be determined. Within this strain range the polymer is strained without destroying its chemical bonds. This is an essential condition for possible mathematical evaluation of the experiments. The maximum possible polymer deformation is $\gamma = 1$. Within the viscoelastic range that was explored, the measured elastic ratios are considerable. The calculated loss factor varies between 1.6 and 2.5, i.e. the viscous ratio increases with increasing styrene content (Table 10).

2.6.2 Curing and pyrolysis

The oxygen curing of poly(carbosilane) (PCS) fibers, according to Eqns [49] and [50], is

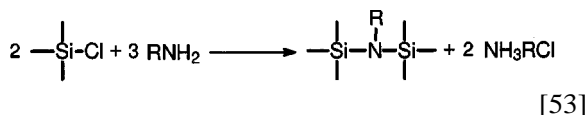
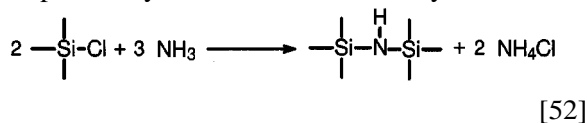
currently being developed on an industrial scale.



The pyrolysis product is a non-stoichiometric combined Si—C—O ceramic fiber, well known as NicalonTM fiber.^{4,133} However, the high oxygen content (≈ 10 wt%) decreases the mechanical fiber properties and especially the thermal resistance, because of the fiber decomposition that occurs with SiO and CO evolution at around 1300 K (Eqn [51]).¹³⁴ These carbothermal reactions are particularly efficient in the presence of excess carbon.



In contrast with oxygen and radiation curing methods Eqn [8], poly(chloromethylsilane-co-styrene) fibers can be rendered infusible by reaction of Si—Cl groups with ammonia (Eqn [52]) or alkylamines (Eqn [53]) leading to a superficially crosslinked silazane layer.¹³⁵



Thus, the introduction of oxygen can be avoided. The structural change in CoP 19 after curing with ammonia was monitored by ²⁹Si CP MAS-NMR spectroscopy (Fig. 15a). In comparison with the

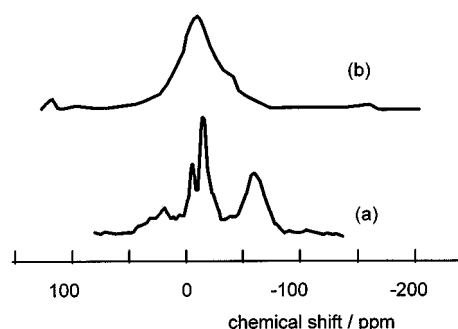


Figure 15 ²⁹Si MAS-NMR spectra of (a) ammonia-cured polysilane at 200 °C and (b) ammonia-cured fiber sample after pyrolysis at 1200 °C.

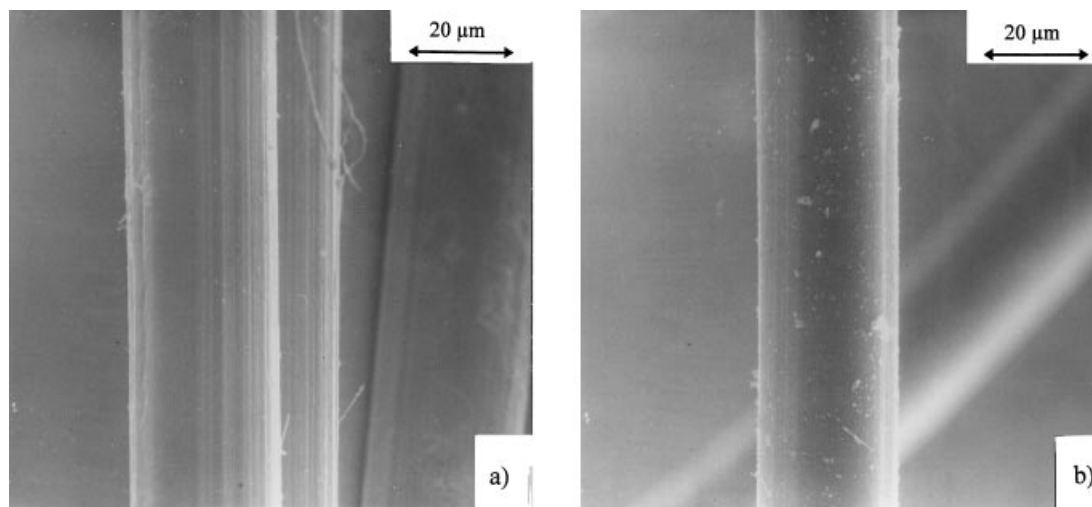


Figure 16 SEM micrographs of SiC fibers from poly(chloromethylsilane-co-styrene) (CoP 18): (a) after pyrolysis at 1200 °C; (b) pyrolyzed fiber after treatment under air at 1400 °C for 30 min.

^{29}Si NMR spectrum of the starting CoP 18 (Fig. 12a), the ^{29}Si NMR spectrum of the cured sample shows resonance signals in the -20 to -40 ppm range. These signals are certainly due to the presence of $\text{SiN}_x\text{C}_{4-x}$ sites.¹³⁶ The terminal $-\text{SiMeCl}_2$ groups (related to the signal around 35 ppm) are completely consumed. This indicates that the ammonolysis is already starting at the terminal units at 90 °C and continues at higher curing temperatures up to 300 °C at the silylene groups $>\text{SiClMe}$ (30–10 ppm).

The level of nitrogen incorporation can be adjusted with the curing temperature. After curing, the preceramic fibers (CoP 18) are converted into nitrogen-containing SiC fibers upon pyrolysis under an inert gas atmosphere. The ^{29}Si NMR spectrum of this sample (Fig. 15b) shows an intense signal around -10 ppm, that can be assigned to SiC_4 sites. A signal of low intensity between -20 and -30 ppm is also present which can be assigned to $\text{SiN}_x\text{C}_{4-x}$ sites.

A nearly constant free carbon content of around 3 wt% was found in all the CoPs (10, 18, 25) investigated after pyrolysis at 1200 °C (1 h). This behavior is explained by favored polystyrene block decomposition and subsequent evaporation during pyrolysis. The ceramic yields of the cured polymers are about 35 wt%, which is rather low. Nevertheless the properties of the SiC fibers derived from CoP 18 (Table 11) demonstrate that ceramic yields do not exclusively determine the final fiber quality.

X-ray investigations prove the amorphous

state of SiC after pyrolysis at 1200 °C.¹³⁷ Nano-crystalline SiC is observed between 1200 and 1500 °C. These crystallite sizes result from fibers which were heated to the stated temperature and then after 30 min cooled to room temperature. The crystallization of β -SiC is retarded by small nitrogen and chlorine contents which are still present in the fibers.

The fibers are heat-resistant up to 1500 °C in air for >1 h. Higher temperatures cause a crystallite growth associated with a drop in the mechanical fiber properties and formation of a thick oxide layer. SEM micrographs of SiC fibers (derived from CoP 18) with a diameter of 25 μm are shown in Fig. 16 (a) and (b). The fiber surface is smooth and no serious defects are observed (a). A SiC fiber treated at 1400 °C under air for 30 min is shown in micrograph (b). Some light spots on the surface are observed which are attributed to an oxide layer starting to develop on the fibers. Such a layer was not noticed after air treatment for the same time at lower temperatures.

3 CONCLUSIONS

The Wurtz-type polymerization of dichloro-, trichloro- or tetrachloro-silanes makes possible synthetic pathways to organosilicon polymer architectures ranging from 1D and 2D to 3D topologies. These architectures are based on

secondary $>\text{SiR}_2$, tertiary $\text{RSi}(\text{Si})_3$ or quaternary $\text{Si}(\text{Si})_4$ silicon units in the polymer backbone. This allows the tailoring of certain polymer properties by control of the polymer architecture; knowledge of how to do this is currently mainly focused on variation of photophysical polymer properties. Dehalocoupling reactions rarely tolerate reactive monomer functionalities apart from halogen substituents. In consequence the latent polymer reactivity is low. The stimulation of the polymer reactivity (thermal treatment, irradiation, chemical modification) demands additional processing steps, which are essential in the manufacture of polymer-derived SiC shaped materials.

By contrast, metallocene-catalyzed dehydropolymerization of organosilanes and organodisilanes provide linear and branched polysilane backbones bearing Si–H functionalities. However, the high reactivity is detrimental to the controlled formation of well-defined linear polysilylenes. The polymers usually have a rather oligomeric character. Subsequent crosslinking can easily be performed by thermal treatment or chemical modification in which Si–H functionalities are consumed. Crosslinked polymers usually show high ceramic yields on pyrolysis.

Heterogeneous Lewis-base catalyzed disproportionation of haloorganodisilanes provides poly(chloromethylsilane)s of 3D polysilyne-type architectures constituted by arrangements of fused rings. In the first stages of the reaction, mainly branched oligosilanes form. The oligosilanes undergo thermally induced branching and crosslinking reactions even in the absence of the catalyst, leading to the formation of poly(chloromethylsilane)s. The polymers are also rather oligomeric. They can be easily crosslinked by thermal treatment or by chemical modification using Si–Cl functionalities.

The disproportionation of halo-organodisilanes in the presence of olefins such as styrene gives polystyrene-containing poly(chloromethylsilane)s, probably with copolymeric character. Investigations concerning the polymer structure are in progress. Nevertheless these polymers have been proved to be excellent precursors for fiber spinning. The polymer fibers are cured under ammonia, and then pyrolyzed to SiC fibers containing small contents of nitrogen ($<5\%$). The SiC fibers exhibit mechanical properties similar to those of commercial SiC fibers. They are resistant in air at temperatures as high as

1500 °C.

The proposed polymerization mechanisms of dehalocoupling, catalytic dehydropolymerization or catalytic disproportionation might be attributed to a common basic initiation step: electron transfer. The electron source may vary: metals, metal complexes or Lewis bases. While during dehalocoupling reactive silylanion intermediates form, dehydropolymerization of disilanes and disproportionation of halodisilanes obviously form silylenes due to Si–Si bond cleavage. The silylenes undergo insertion on silicon sites bearing functional groups (Si–H, Si–Cl). This conclusion is supported by the analogous spectra of reaction products consisting of branched oligomers and polymers. The coordinative stabilization of the silylenes formed is provided by the presence of the metal complex or Lewis bases.

4 EXPERIMENTAL

4.1 Synthesis

4.1.1 Synthesis of oligo- and poly-(chloromethylsilane)s from $\text{MeCl}_2\text{Si-SiCl}_2\text{Me}$

All glass apparatus was carefully dried and flushed with argon. The synthesis apparatus is shown in Fig. 17. A 500-ml three-necked flask (A) was equipped with a magnetic stirrer, a thermoelement inlet, an inert gas inlet and a distilling link with a drain stopcock. A 25 cm \times 10 cm column (B) was placed on the distilling link. A second distilling link with a drain stopcock was equipped with a reflux condenser (C) and placed on top of column (B). The drain stopcocks were both connected with 250 ml flasks for collecting the volatile reaction products. The system was closed hydraulically by two wash bottles filled with silicone oil. The column (B) was filled with 10 g of catalyst [bis(dimethylamido)phosphoryl groups grafted onto a silica surface] mixed with Raschig rings.

Flask (A) was charged with 250 ml of **2** heated to boiling point. Supported by the argon stream (3 l h^{-1}), the gaseous **2** was carried to the catalyst. The start of disproportionation could be recognised by the formation of bubbles on the catalyst surface, caused by the formation of MeSiCl_3 . The reaction system was heated at reflux until the temperature above the catalyst became constant ($64\text{--}65\text{ }^\circ\text{C}$). The MeSiCl_3 formed was continuously removed by reducing

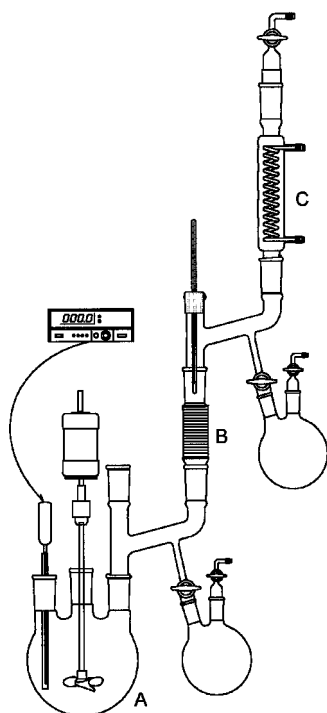


Figure 17 Apparatus for the catalytic disproportionation of halodisilanes.

reflux. The oligomers formed flowed back to the flask (A) and were enriched as the reaction temperature increased. If the reaction was interrupted at 170–175 °C an oligosilane mixture consisting of the chloromethyloligosilanes **3–7** and small amounts of unreacted **2** and MeSiCl_3 could be obtained. By further increase of the reaction temperature, polymers were formed from the oligomer mixture. The composition as well as the meltability and solubility of the polymers depend on the reaction temperature and time. In general, the polymers obtained up to 250 °C were soluble in common organic solvents such as toluene, chloroform or THF. Higher temperatures led to insoluble and unmelttable products. Two examples of the polysilanes that have been prepared are given in Table 12.

4.1.2. Synthesis of poly(chloromethylsilane-co-styrene)s

The poly(chloromethylsilane-co-styrene)s were prepared according to the procedure described in Section 4.1.1, using the various starting mixtures of $\text{MeCl}_2\text{Si—SiCl}_2\text{Me}$ (**2**) and styrene (C_8H_8) shown in Table 13. The final reaction temperature of 220 °C was held for 2 h.

4.2 NMR experiments

The spectra were recorded on a Bruker MSL300 spectrometer with a Bruker CP-MAS probe using 7 mm ZrO_2 rotors. All the rotors were filled in a glove-box under a dry argon atmosphere. The spinning rate was 5 kHz. All the experiments, CP and IRCP, were performed under the same Hartmann–Hahn conditions with both RF channel levels set at about 42 kHz. Details of the CP and IRCP experiments have been given elsewhere.¹²³ The FIDs were analyzed with the WIN-NMR Bruker program and the spectra were simulated with the WIN-FIT program.¹³⁸

4.3 Computational details

All molecular structures were optimized at the restricted Hartree–Fock level (RHF) with the 3–21G(*) basis set. Minima were verified by establishing that the matrices of the energy second derivatives have zero eigenvalue. The calculations were done with *Spartan 3.1*¹³⁹ and *GameSS*.¹⁴⁰

4.4 Rheology

Rheological measurements were carried out under an inert gas atmosphere (argon), with a UM/MC20 viscosimeter equipped with a cone/plate system (cone angle, 0.5 °; radius, 25 mm) (Physica Company, Stuttgart, Germany).

4.5 Melt spinning of poly(chloromethylsilane-co-styrene)s

All apparatus was carefully dried and rinsed with argon. CoPs 10, 18, 25 were melted under an argon atmosphere in a melting flask. The flask was connected with a tube by a stopcock over which the polymer melt was filled into the spinning head. The spinning head was connected with a glove box by a glass tube. The polymer was extruded through a multi-hole spinneret (200 filaments) by argon pressure (20–30 bar). Once spun, the polymer filaments were immediately stretched out to diameters of 15–40 μm by winding on a bobbin placed in the glove box.

4.6 Curing of pre-ceramic fibers

The continuous green filaments wound on a bobbin were put in a vessel made of stainless steel. At the beginning of the curing process the

temperature should not exceed 30 K below the melting region to avoid the filaments sticking together. The filaments were cured (5 l h^{-1}) in a stream of a mixture of 90 vol% argon and 10 vol% ammonia. The filaments were held at a temperature of 300 °C (maximum) for 15 min.

4.7 Pyrolysis

The pyrolysis of the cured pre-ceramic filaments was performed in an alumina tube furnace (HTM). The filaments, 5 cm in length, were transferred into an alumina tube in a glove box. The closed tube was subsequently inserted into the furnace tube. The filaments were heated at 50 K min^{-1} to 1200 °C and held for 10 min under a slow stream of argon (3 l h^{-1}).

Acknowledgements We gratefully acknowledge the financial support of the Deutsche Forschungsgemeinschaft (Ro 961/4-2, Mu 943/6-2) and the 'Fonds der chemischen Industrie', and also NATO for a collaborative grant between the Universities of Paris and Freiberg.

REFERENCES

1. S. Yajima, J. Hayashi and M. Omori, *Chem. Lett.* 931 (1975).
2. S. Yajima, J. Hayashi, M. Omori and K. Okamura, *Nature (London)* **261**, 683 (1976).
3. R. Laine and F. Babonneau, *J. Chem. Mater.* **5**, 260 (1993) and references cited therein.
4. S. Yajima, in: *Handbook of Composites*, Vol. 1, Strong Fibers, Watt, W. and Prerov, D. V. (eds), Elsevier Science, Amsterdam, 1985, pp. 202–236.
5. R. M. Laine, Z.-F. Zhang, K. W. Chew, M. Kannisto and C. Scotto, in: *Ceramic Processing Science and Technology*, Hausner, H., Messing, G. and Hirano, S. (eds), Am. Ceram. Soc., Westerville, OH, USA, 1995, pp. 179–186.
6. T. Ishikawa, *Comp. Sci. Tech.* **51**, 135 (1994).
7. J. F. Harrod, in: *Inorganic and Organometallic Polymers*, Zeldin, M., Wynne, K. J. and Allcock, H. R. (eds), American Chemical Society, ACS Symp. Ser. No. 360, Washington DC, 1988, p. 89.
8. T. D. Tilley, *Acc. Chem. Res.* **26**, 22 (1993).
9. Z. F. Zhang, F. Babonneau, R. M. Laine, Y. Mu, J. F. Harrod and J. A. Rahn, *J. Am. Ceram. Soc.* **74**, 670 (1991).
10. E. Hengge, in: *Organosilicon Chemistry*, Part I, Auner, N. and Weis, J. (eds), VCH, Weinheim, 1994, 280.
11. E. Hengge and M. Weinberger, *J. Organomet. Chem.* **433**, 21 (1992).
12. E. Hengge and M. Weinberger, *J. Organomet. Chem.* **443**, 167 (1993).
13. R. H. Baney, J. H. Gaul and T. K. Hilty, *Organometallics* **2**, 859 (1983).
14. R. D. Miller and J. Michl, *Chem. Rev.* **89**, 1359 (1989) and references cited therein.
15. R. West and J. Maxka, in: *Inorganic and Organometallic Polymers*, Zeldin, M., Wynne, K. J. and Allcock, H. R. (eds), American Chemical Society, ACS Symp. Ser. No. 360, Washington DC, 1988, Chapter 2.
16. K. Matyjaszewski, Y. L. Chen and H. K. Kim, in: *Inorganic and Organometallic Polymers*, Zeldin, M., Wynne, K. J. and Allcock, H. R. (eds), American Chemical Society, ACS Washington DC, 1988, Chapter 6.
17. D. J. Worsfold, in: *Inorganic and Organometallic Polymers*, Zeldin, M., Wynne, K. J. and Allcock, H. R. (eds), American Chemical Society, ACS Symp. Ser. No. 360, Washington DC, 1988, Chapter 8.
18. K. Matyjaszewski, *J. Inorg. Organomet. Polym.* **1**, 463 (1991).
19. R. West, *J. Organomet. Chem.* **300**, 327 (1986).
20. R. West, in: *Inorganic Polymers*, Polymer Science and Engineering Series, Prentice Hall, New Jersey, 1992, pp. 186–236.
21. R. West, in: *Comprehensive Organometallic Chemistry*, Wilkinson, G., Stone, F. G. A. and Abel, E. (eds), Pergamon, Oxford, 1982, Chapter 9.4, pp. 365–397.
22. J. Maxka, J. Chrusciel, M. Sasaki and K. Matyjaszewski, *Macromol Symp.* **77**, 79 (1994).
23. K. Matyjaszewski, D. Greszta, J. S. Hrkach and H. K. Kim, *Macromolecules* **28**, 59 (1995).
24. A. Watanabe, H. Miike, Y. Tsutsumi and M. Matsuda, *Macromolecules* **26**, 2111 (1993).
25. N. Auner, R. Probst, F. Hahn and E. Herdtweck, *J. Organomet. Chem.* **459**, 25 (1993).
26. R. G. Jones, R. E. Benfield, P. J. Evans and A. C. Swain, *J. Chem. Soc., Chem. Commun.* **14**, 1465 (1995).
27. B. Lacave-Goffin, L. Hevesi and J. Devaux, *J. Chem. Soc., Chem. Commun.* **4**, 769 (1995).
28. M. Fujino and N. Matsumoto, *J. Polym. Sci., Part C: Polym. Lett.* **26**, 109 (1988).
29. R. Menescal, R. West and M. Blazsó, *J. Inorg. Organomet. Polym.* **5**, 217 (1995).
30. P. A. Bianconi and T. W. Weidman, *J. Am. Chem. Soc.* **110**, 2342 (1988).
31. P. A. Bianconi and T. W. Weidman, *Macromolecules* **22**, 1697 (1989).
32. K. Matyjaszewski, J. Chrusciel, J. Maxka and M. Sasaki, *J. Inorg. Organomet. Polym.* **5**, 261 (1995).
33. J. B. Lambert, J. L. Pflug and C. L. Stern, *Angew. Chem.* **107**, 106 (1995).
34. A. Sekiguchi, M. Nanjo, C. Kabuto and H. Sakurai, *J. Am. Chem. Soc.* **117**, 4195 (1995).
35. W. Uhlig, *Z. Naturforsch. Teil B* **50**, 1674 (1995).
36. E. Orti, R. Crespo, M. C. Piqueras, F. Tomas and J. L. Brédas, *Synth. Metals* **55–57**, 4419 (1993).
- 36a. R. Crespo, M. C. Piqueras, E. Orti and J. L. Brédas, *Synth. Metals* **43**, 3457 (1991).
37. K. Furukawa, M. Fujino and N. Matsumoto, *Macro-*

- molecules **23**, 3423 (1990).
38. M. Sasaki and K. Matyjaszewski, *J. Polym. Sci. Part A: Polym. Chem.* **33**, 771 (1995).
 39. M. Matyjaszewski and H. K. Kim, *Polym. Bull.* **22**, 253 (1989).
 40. C. L. Schilling, J. P. Wesson and T. C. Williams, *Am. Ceram. Soc. Bull.* **62**, 912 (1983).
 41. Y.-T. Shieh and S. P. Sawan, *J. Appl. Polym. Sci.* **58**, 2013 (1995).
 42. W. R. I. Cranstone, S. M. Bushnell-Watson and J. H. Sharp, *J. Mater. Res.* **10**, 2659, (1995).
 43. K. Busch, R. Richter and G. Roewer, unpublished results.
 44. W. Toreki, C. D. Batich, M. D. Sacks and A. A. Morrone, *Ceram. Eng. Sci. Proc.* **11**, 198 (1992).
 45. K. Shiina and M. Kumada, *J. Organomet. Chem.* **23**, 139 (1958).
 46. S. Yajima, Y. Hasegawa, J. Hayashi and M. Imura, *J. Mater. Sci.* **13**, 2569 (1978).
 47. I. M. T. Davidson, *J. Organomet. Chem.* **341**, 255 (1988).
 48. M. Birot, J.-P. Pillot and J. Dunoguès, *Chem. Rev.* **95**, 1443 (1995).
 49. M. Ishikawa and M. Kumada, *Adv. Organomet. Chem.* **19**, 51 (1981).
 50. R. West, A. R. Wolff and D. J. Peterson, *J. Rad. Curing* **13**, 35 (1986).
 51. R. D. Miller, D. Hofer, J. F. Rabolt, R. Sooriyakumaran, C. G. Wilson, G. N. Ficks and J. E. Guillet, in: *Polymers for High Technology: Electronics and Photonics*, Bowden, M. J. and Turner, S. R. (eds), American Chemical Society, ACS Symp. Ser. No. 346, Washington DC, 1984, Chapter 14.
 52. S. Gauthier and D. J. Worsfold, *Macromolecules* **22**, 2213 (1989).
 53. R. West, L. D. David, P. I. Djurovich, K. S. V. Srinivasan and H. Yu, *J. Am. Chem. Soc.* **103**, 7352 (1981).
 54. M. Takeda, Y. Imai, H. Ichikawa, T. Ishikawa, T. Seguchi and K. Okamura, *Ceram. Eng. Sci. Proc.* **12**(7–8), 1007 (1991).
 55. M. Takeda, Y. Imai, H. Ichikawa, T. Ishikawa, N. Kasai, T. Seguchi and K. Okamura, *Ceram. Eng. Sci. Proc.* **13**(7–8), 209 (1992).
 56. M. Takeda, Y. Imai, H. Ichikawa, T. Ishikawa, N. Kasai, T. Seguchi and K. Okamura, *Ceram. Eng. Sci. Proc.* **14**(9–10), 540 (1993).
 57. M. Takeda, J. Sakamoto, Y. Imai, H. Ichikawa and T. Ishikawa, *Ceram. Eng. Sci. Proc.* **15**, 133 (1994).
 58. M. Sugimoto, T. Shimoo, K. Okamura and T. Seguchi, *J. Am. Ceram. Soc.* **78**, 1013 (1995).
 59. M. Sugimoto, T. Shimoo, K. Okamura and T. Seguchi, *J. Am. Ceram. Soc.* **78**, 1849 (1995).
 60. K. Okamura and T. Seguchi, *J. Inorg. Organomet. Polym.* **2**, 171 (1992).
 61. K. Okamura, M. Sato, T. Seguchi and S. Kawaniski, in: *Controlled Interphases in Composite Materials*, Elsevier Science, Amsterdam, 1990, pp. 209–218.
 62. C. L. Schilling and T. C. Williams, *Am. Chem. Soc., Polym. Prepr.* **1**, 25 (1984).
 63. C. L. Schilling Jr, *Br. Polym. J.* **18**, 355 (1986).
 64. D. Seyferth, C. A. Sobon and J. Borm, *New J. Chem.* **14**, 545 (1989).
 65. D. Seyferth and Y.-F. Yu, US Patent 4 639 501 (1987).
 66. B. Boury, L. Carpenter and R. J. P. Corriu, *Angew. Chem., Int. Ed. Engl.* **29**, 785 (1990).
 67. B. Boury, R. J. P. Corriu, D. Leclercq, P. H. Mutin, J. M. Planeix and A. Vioux, *Organometallics* **10**, 1457 (1991).
 68. B. Boury, R. J. P. Corriu and W. E. Douglas, *Chem. Mater.* **3**, 487 (1991).
 69. R. Riedel, A. Kienzle, V. Szabo and J. Mayer, *J. Mater. Sci.* **28**, 3931 (1993).
 70. A. F. Diaz and R. D. Miller, *J. Electrochem. Soc.* **132**, 834 (1985).
 71. H. Bock, *Angew. Chem.* **101**, 1659 (1989).
 72. W. Habel, L. Mayer and P. Sartori, *Chem.-Ztg* **115**, 301 (1991).
 73. W. Habel, L. Mayer and P. Sartori, *Chem.-Ztg* **115**, 117 (1991); **115**, 301 (1991).
 74. M. Ishikawa, M. Kumada and H. Sakurai, *J. Organomet. Chem.* **23**, 63 (1970).
 75. E. Bacqué, J.-P. Pillot, M. Birot, J. Dunoguès and P. Lapouyade, *Chem. Mater.* **3**, 348 (1991).
 76. M. Kumada and K. Tamao, *Adv. Organomet. Chem.* **6**, 19 (1968).
 77. H. Watanabe, M. Kobayashi, Y. Koike, S. Nagashima and Y. Nagai, *J. Organomet. Chem.* **128**, 173 (1977).
 78. W. Habel, A. Oelschläger and P. Sartori, *J. Organomet. Chem.* **486**, 267 (1995).
 79. W. Habel, A. Oelschläger and P. Sartori, *J. Organomet. Chem.* **494**, 157 (1995).
 80. Unpublished results; the ethynyl-containing polymers were melt-spun in the author's laboratories.
 81. R. Richter, H. P. Martin, G. Roewer, E. Müller, H. Krämer, P. Sartori, A. Oelschläger, W. Habel and B. Harnack, European Patent, EP 0 668 254 A2 (1995).
 82. F. Yenca, Y. L. Chen and K. Matyjaszewski, *Polym. Prepr.* **28**, 222 (1987).
 83. K. E. Ruehl and K. Matyjaszewski, *J. Organomet. Chem.* **410**, 1 (1991).
 84. W. Uhlig, *J. Organomet. Chem.* **469**, C1 (1994).
 85. A. R. Bassingdale and T. Stout, *J. Organomet. Chem.* **271**, C1 (1984).
 86. C. Tretner, B. Zobel, R. Hummeltenberg and W. Uhlig, *J. Organomet. Chem.* **468**, 63 (1994).
 87. W. Uhlig, (a) *J. Organomet. Chem.* **402**, C45 (1991); (b) *Chem. Ber.* **125**, 47 (1992); (c) *J. Organomet. Chem.* **456**, C1 (1993).
 88. W. Uhlig, *J. Polym. Sci.: Part A: Polym. Chem.* **33**, 239 (1995).
 89. H. Emde, D. Domsch, H. Feger, U. Frick, A. Götz, H. Hergott, K. Hoffmann, W. Kober, K. Krägeloh, T. Oesterle, W. Steppan, W. West and G. Simchen, *Synthesis* **1** (1982).
 90. W. Uhlig and C. Tretner, *J. Organomet. Chem.* **467**, 31 (1994).

91. P. Sartori and W. Habel, *J. Prakt. Chem.* (1996) and references cited therein (in press).
92. (a) C. Aitken, J. F. Harrod and E. Samuel, *J. Organomet. Chem.* **279**, C11 (1985); (b) C. Aitken, J. F. Harrod and E. Samuel, *J. Am. Chem. Soc.* **108**, 4059 (1986); (c) C. Aitken, J. F. Harrod and E. Samuel, *Can. J. Chem.* **64**, 1677 (1986); (d) J. F. Harrod and S. S. Yun, *Organometallics* **6**, 1381 (1987); (e) Y. Mu and J. F. Harrod, in: *Inorganic and Organometallic Oligomers and Polymers*, IUPAC 33rd Symposium on Macromolecules, Harrod, J. F. and Laine, R. M. (eds), Kluwer, Dordrecht, 1991, pp. 23–36; (f) J. F. Harrod, in: *Inorganic and Organometallic Polymers with Special Properties*, NATO ASI Ser. E: Appl. Sci. Vol. 206, Laine, R. M. (ed.), Kluwer Dordrecht, 1991, pp. 127–146.
93. H.-G. Woo, J. F. Walzer and T. D. Tilley, *J. Am. Chem. Soc.* **114**, 7047 (1992).
94. H. Yamashita and M. Tanaka, *Bull. Chem. Soc. Jpn.* **68**, 403 (1995) and references cited therein.
95. D. Seyferth, M. Tasi and H.-G. Woo, *Chem. Mater.* **7**, 236 (1995).
96. D. Seyferth and D. Y. Son, *Bull. Soc. Chem. Fr.* **132**, 489 (1995).
97. U. Herzog, R. Richter, E. Brendler and G. Roewer, *J. Organomet. Chem.* **507**, 221 (1996).
98. R. F. Trandell and G. Urry, *J. Inorg. Nucl. Chem.* **40**, 1305 (1978).
99. G. Urry, *J. Inorg. Nucl. Chem.* **26**, 409 (1964).
100. A. Kaczmarczyk and G. Urry, *J. Am. Chem. Soc.* **82**, 751 (1960).
101. D. Kummer, A. Balkir and H. Köster, *J. Organomet. Chem.* **178**, 29 (1979).
102. G. Sawitzki and H. G. v. Schnering, *Chem. Ber.* **109**, 3728 (1976).
103. D. Kummer and H. Köster, *Angew. Chem.* **81**, 897 (1969).
104. D. Kummer, H. Köster and M. Speck, *Angew. Chem.* **81**, 574 (1969).
105. D. Kummer, S. C. Chaudhry, W. Depmeier and G. Mattern, *Chem. Ber.* **123**, 2241 (1990).
106. General Electric Co. (A. R. Gilbert and G. D. Cooper), US Patent 2 842 580 (1955).
107. G. D. Cooper and A. R. Gilbert, *J. Am. Chem. Soc.* **82**, 5042 (1960).
108. J. V. Urenovitch, R. Pejic and A. G. McDiarmid, *J. Chem. Soc.* **85**, 5563 (1963).
109. J. V. Urenovitch and A. G. McDiarmid, *J. Am. Chem. Soc.* **85**, 3372 (1963).
110. R. Calas, J. Dunoguès, G. Deleris and N. Duffaut, *J. Organomet. Chem.* **225**, 117 (1982).
111. R. Calas, N. Duffaut and R. Puthet French Patent 1 507 272 (1966).
112. J. Albrecht, R. Richter and G. Roewer, German Patent DE 42 07 229 A 1 (1992).
113. R. Richter, N. Schulze, G. Roewer and J. Albrecht, *J. Prakt. Chem.* (1996) (accepted for publ.).
114. R. Richter, Ph.D. Thesis, TU Bergakademie Freiberg, Germany, 1995.
115. V. K. Turchanikov, K. B. Petrushenko, A. I. Vokin, A. F. Jermikov, L. A. Jeskova, L. V. Baikalova and J. S. Domnina, *Zh. Org. Khim.* **25**, 1138 (1989).
116. A. M. Koulkes-Pujo, L. Gilles, B. Lesigne and J. Sutton, *J. Chem. Soc., Chem. Commun.* **71**, (1994).
117. (a) T. Clark, in: *A Handbook of Computational Chemistry*, J. Wiley, New York, 1988; (b) W. J. Hehre, in: *Practical Strategies for Electronic Structure Calculations*, Wavefunction Inc., Irvine, CA, 1995.
118. W. H. Atwell and D. R. Weyenberg, *Angew. Chem.* **81**, 485 (1969).
119. J. Heinicke, B. Gehrhuss and S. Meinel, *J. Organomet. Chem.* **474**, 71 (1994).
120. Y. Kimata, H. Suzuki, S. Satoh and A. Kuriyama, *Organometallics* **14**, 2506 (1995).
121. H.-G. Woo, S.-Y. Kim, M.-K. Han, E. J. Cho and I. N. Jung, *Organometallics* **14**, 2415 (1995).
122. F. Babonneau, C. Bonhomme, R. Richter and G. Roewer, *J. Chim. Phys.* **92**, 1745 (1995).
123. F. Babonneau, C. Bonhomme, R. Richter, G. Roewer and D. Balhoul, *Chem. Mater.* **8**, 1415–1428 (1996).
124. X. Wu and K. W. Zlim, *J. Magn. Res. A* **102**, 205 (1993).
125. R. Sangill, N. Rastrup-Andersen, H. Bildsoe, H. J. Jacobsen and N. C. Nielsen, *J. Magn. Res. A* **107**, 67 (1994).
126. A. Pines, M. G. Gibby and J. S. Waugh, *J. Chem. Phys.* **59**, 569 (1973).
127. Dr. Weyenberg, L. H. Toporcer and A. E. Bey, *J. Org. Chem.* **30**, 4096 (1965).
128. C. L. Schilling and T. C. Williams, *Organosilane Polymers*, V1th ORN Technical Report 83-2.
129. T. Adrian, W. Habel and P. Sartori, *Chem.-Ztg* **115**, 1 (1991).
130. B. v. Aefferden, W. Habel and P. Sartori, *Chem.-Ztg* **114**, 259 (1990); **114**, 309 (1990).
131. M. Weidenbruch, *Coord. Chem. Rev.* **130**, 275 (1994).
132. A. Ziabicki, in: *Fundamentals of Fibre Formation*, Wiley, London, 1976.
133. Y. Hasegawa and K. Okamura, *J. Mater. Sci.* **18**, 3633 (1983).
134. T. Shimoo, K. Okata, M. Narisawa and K. Okamura, *J. Ceram. Soc. Jap., Int. Ed.* **102**, 952 (1994).
135. (a) R. Richter, G. Roewer, E. Brendler, H. Krämer, H.-P. Martin and E. Müller, in: *Advanced Structural Fiber Composites*, Vicenzini, P. (ed), Advances in Science and Technology, Vol. 7, Techna, Faenza, Italy, 1995, pp. 45–52; (b) H.-P. Martin, R. Richter, E. Müller, G. Roewer and E. Brendler, in: *Advanced Structural Fiber Composites*, Vicenzini, P. (ed), Advances in Science and Technology, Vol. 7, Techna: Faenza, Italy, 1995; pp. 53–60.
136. N. Brodie, J.-P. Majoral and J.-P. Disson, *Inorg. Chem.* **32**, 4646 (1993).
137. H.-P. Martin, R. Richter, E. Brendler, E. Müller and G. Roewer, *Proc. ICCM 10*, Vol 6, *Microstructure, Degradation and Design*, Poursartip, A. and Street, K.

-
- (eds), The Tenth International Conference on Composite Materials Society, Woodhead, Vancouver, Canada, 1995, p. 307.
138. D. Massiot, H. Thiele and A. Germanus, *Bruker Rep.* **140**, 43 (1994).
139. *Spartan 3.1*, Wavefunction Inc., Irvine, CA, 1993.
140. *GameSS*, Iowa State University; described in *QCPE Bulletin* **10**, 52 (1990).